Profitability of energy arbitrage net profit for grid-scale battery energy storage considering dynamic efficiency and degradation using a linear, mixed-integer linear, and mixed-integer

Journal of Energy Storage 95 (2024) 112380

Contents lists available at ScienceDirect

Journal of Energy Storage

journal homepage: www.elsevier.com/locate/est

Research papers

Profitability of energy arbitrage net profit for grid-scale battery energy storage considering dynamic efficiency and degradation using a linear, mixed-integer linear, and mixed-integer non-linear optimization approach

Alberto Grimaldi [a,b,c,*], Francesco Demetrio Minuto [a,b], Jacob Brouwer [c], Andrea Lanzini [a,b]

[a] Department of Energy, Politecnico di Torino, Corso Duca degli Abruzzi 24, 10129 Torino, Italy
[b] Energy Center Lab, Politecnico di Torino, Via Paolo Borsellino 38/16, 10138 Torino, Italy
[c] Clean Energy Institute, University of California, Irvine, CA 92697-3550, United States of America

ARTICLE INFO

Keywords:
Grid-scale battery energy storage
Energy arbitrage
Electricity markets
Battery degradation
Battery lifetime
MILP optimization

ABSTRACT

Grid-scale energy storage is becoming an essential element to effectively support the rapid increased use of renewable energy sources in the power network. The present work proposes a long-term techno-economic profitability analysis considering the net profit stream of a grid-level battery energy storage system (BESS) performing energy arbitrage as a grid service. The net profit is a cost function that includes the revenue derived by arbitrage, the import cost and the degradation cost induced by battery capacity fade. Three optimization techniques with a computationally efficient optimization logic are developed. The scenario with no-degradation is formulated as a linear programming (LP) problem, while the scenarios with and without degradation are formulated as mixed-integer linear programming (MILP), and as mixed-integer non-linear programming (MINLP) problems. The non-linearity is introduced by implementing a BESS dynamic charge/discharge efficiency that is a function of the BESS power rate. Based on the obtained BESS optimal scheduling, a long-term profitability analysis is developed during the whole BESS lifetime. In the proposed case study, historical electricity market prices from the CAISO electricity market in the United States, California, are used as input. We found that, even without degradation, the break-even investment cost that makes the BESS profitable with a power to-energy-ratio of 1 MW/2MWh is 210 $/kWh. By implementing a cycle-counting degradation model, we observed a remarkable battery degradation on BESS profitability corresponding to a yearly net profit reduction in the 13–24 % range. From a long-term application perspective, the BESS calendar lifetime could be extended by reducing the battery cycling. Such cycling reduction is obtained by adding a penalty cost in the objective function of the energy arbitrage optimization problem.

1. Introduction

In the modern power network, battery energy storage systems (BESS) are playing a crucial role as low-carbon flexible resources, due to their ability to address renewable energy intermittency [1] and to provide a wide range of grid services (e.g., energy arbitrage, frequency regulation, load-shifting) [2].

Energy storage deployment in electricity markets has been steadily increasing in recent years. In the U.S., from 2003 to 2019, 1044 MW power capacity of large-scale battery storage was installed, and an additional 10,000 MW is likely to be installed between 2021 and 2023, 10 times the total amount of maximum generation capacity by all systems in 2019 [3]. Almost one-third of U.S. large-scale battery storage additions will come from CAISO[1] and PJM[2] grid operators [3]. As of October 2022, 7.8 GW of utility-scale battery storage was operating in the United States. From 2023 to 2025, developers and power plant operators expect to add another 20.8 GW of battery storage capacity [4]. More than 75 % of the 20.8 GW of utility-scale battery capacity that owners and operators reported that they plan to install from 2022 to 2025 is located in Texas (7.9 GW) and California (7.6 GW) [4]. Concerning the BESS capital cost, as reported by IEA World Energy Outlook 2023 [5], the capital cost of utility-scale stationary batteries will have to decrease from 315 $/kWh in 2022 to 185 $/kWh in 2030, and to 140

* Corresponding author at: DENERG, Politecnico di Torino, Corso Duca degli Abruzzi 24, 10129 Torino, Italy.
E-mail address: alberto_grimaldi@polito.it (A. Grimaldi).

[1] CAISO (California Independent System Operator) is a non-profit Independent System Operator serving California.

[2] PJM (Pennsylvania-New Jersey-Maryland Interconnection) is a regional transmission organization in the United States, part of the Eastern Interconnection grid.

https://doi.org/10.1016/j.est.2024.112380
Received 11 January 2024; Received in revised form 21 May 2024; Accepted 29 May 2024
Available online 14 June 2024

Nomenclature

Abbreviations

BESS	battery energy storage system
CAISO	California independent system operator
EOL	end of life
LMP	locational marginal price
LP	linear programming
MILP	mixed-integer linear programming
MINLP	mixed-integer non-linear programming
SOC	state of charge

LP BESS energy arbitrage model (sets and index)

T	set of optimization time steps [h]
t	index of the optimization time steps

Parameters

Δt	time interval of the optimization problem [h]
E_{nom}^{bess}	BESS nominal capacity [MWh]
P_{nom}^{bess}	BESS nominal power [MW]
η_{ch}	battery charge efficiency [−]
η_{dh}	battery discharge efficiency [−]
$\eta_{inv,LP}$	inverter efficiency [−]
η_{tr}	transformer efficiency [−]
$\eta_{BESS,ch,LP}$	BESS charge efficiency [−]
$\eta_{BESS,dh,LP}$	BESS discharge efficiency [−]

Variables

$P_{ch,LP}^{bess}(t)$	BESS charge power in period t [MW]
$P_{dh,LP}^{bess}(t)$	BESS discharge power in period t [MW]
$SOC_{LP}(t)$	BESS state of charge in period t [MWh]
$\mathbb{P}_{LP}(t)/\mathbb{P}_{n}^{cum}$	profit in period t and its cumulative value [$]
$\mathbb{R}_{LP}(t)/\mathbb{R}_{LP}^{cum}$	export revenue in period t and its cumulative value [$]
$\mathbb{C}_{imp,LP}(t)/\mathbb{C}_{imp,LP}^{cum}$	import cost in period t and its cumulative value [$]
$\lambda_{LMP}(t)$	LMP energy price in period t [$/MWh]

MILP/MINLP BESS energy arbitrage model (sets and indices)

T	set of optimization time steps [h]
t	index of the optimization time steps

Parameters

Δt	time interval of the optimization problem [h]
j	episode considered to evaluate the degradation coefficient [−]
E_{nom}^{bess}	BESS nominal capacity [MWh]
P_{nom}^{bess}	BESS nominal power [MW]
η_{ch}	battery charge efficiency [−]
η_{dh}	battery discharge efficiency [−]
$\eta_{inv,MILP}$	inverter efficiency [−]
η_{tr}	transformer efficiency [−]
$\eta_{BESS,ch,MILP}$	BESS charge efficiency [−]
$\eta_{BESS,dh,MILP}$	BESS discharge efficiency [−]
$\eta_{self-ch}$	self-discharge losses during charge operations [%/h]
$\eta_{self-dh}$	self-discharge losses during discharge operations [%/h]
$\eta_{self-idle}$	self-discharge losses during idle operations [%/h]
T_{BESS}	BESS calendar lifetime [years]
EOL	BESS end of life [fraction of initial capacity]
P_{grid}^{lim}	grid power limit [MW]
$\mathbb{C}_{pen}^{bess}$	degradation penalty cost [$/MWh]
i	interest rate [−]
γ	yearly battery cost escalation rate [−]
$bigM$	bigM method constant

Variables

$P_{ch}^{bess}(t)$	BESS charge power in period t [MW]
$P_{dh}^{bess}(t)$	BESS discharge power in period t [MW]
$SOC(t)$	BESS state of charge in period t [MWh]
$Cyc_{rate}(t)$	BESS fractional cycle rate in period t [−]
Cyc_{rate}^{cum}	BESS cumulative fractional cycle rate in period t [−]
$\eta_{inv}(t)$	inverter dynamic efficiency in period t [−]
$\eta_{BESS,ch}(t)$	BESS dynamic charge efficiency in period t [−]
$\eta_{BESS,dh}(t)$	BESS dynamic discharge efficiency in period t [−]
$\beta_{ch}(t)$	Boolean charge indicator in period t [0,1]
$\beta_{dh}(t)$	Boolean discharge indicator in period t [0, 1]
$\mathbb{P}(t)/\mathbb{P}_{n}^{cum}$	profit in period t and its cumulative value [$]
$\mathbb{R}(t)/\mathbb{R}^{cum}$	export revenue in period t and its cumulative value [$]
$\mathbb{C}_{imp}(t)/\mathbb{C}_{imp}^{cum}$	import cost in period t and its cumulative value [$]
$\mathbb{C}_{deg}(t)/\mathbb{C}_{deg}^{cum}$	degradation cost in period t and its cumulative value [$]
$\mu_{deg,j}$	degradation coefficient evaluated during the episode j [$/MWh]
$E_{start,j}^{rem}$	BESS remaining capacity at the start point of the episode j [%]
$E_{end,j}^{rem}$	BESS remaining capacity at the end point of the episode j [%]
$P_{tot}^{bess}(t)$	sum between the BESS charge and discharge power at time t [MW]
$E_{rem,e}^{bess}(cyc)$	BESS remaining capacity function of the number of cycles [%]
NPV	net present value [$]
NPV_{norm}	normalized net present value [$/MWh]
$P_{rate}(t)$	BESS power rate in period t [−]

$/kWh in 2050. While, according to a recent analysis conducted by NREL [6], the capital cost of a complete 4-hour battery system will decrease from 482 $/kWh in 2022 to 226 $/kWh in 2050.

Although BESS can provide several grid applications, energy arbitrage represents the largest profit opportunity for BESS in the electric power grid [7]. The basic principle of economic energy arbitrage is to generate revenue by charging the battery under low-price conditions and discharging back to the electric grid when prices are higher. According to the U.S. EIA annual electric generator report [8], during 2021, 59 % of the 4.6 GW of utility-scale U.S. battery capacity was used for price arbitrage, up from 17 % in 2019. Considering the U.S. wholesale electricity markets, >80 % of the battery capacity added in 2021 in the CAISO service territory was used for price arbitrage. In fact, as reported by the CAISO special report on battery storage [9], the largest positive revenue comes from day-ahead market energy schedules. For this reason, it is crucial to properly analyze the profitability of using BESS for energy arbitrage grid applications.

1.1. Literature review

In this perspective, there is a growing body of literature on BESS energy arbitrage modelling [7,10–12]. Compared to the voltage-current and concentration-current, the power-energy battery models are the most popular models to characterize the operation of BESS in techno-economic studies [2]. Assumptions about battery efficiency, battery lifetime and degradation are a key challenge to obtain realistic evaluations of profitability.

However, as reported by the complete review of Vykhodtsev et al.

[2], only a limited number of studies have addressed, in detail, the issues about considering a dynamic efficiency and a cycle-counting degradation model into a linear and non-linear optimization framework. One exception is the study conducted by Hesse et al. [13], where the battery dispatch for arbitrage markets is based on a computationally efficient implementation of a mixed-integer linear programming method, with a cost function that includes variable-energy conversion losses and a cycle-induced battery capacity fade. They highlighted the significance of considering both ageing and efficiency in battery system dispatch optimization. However, the impact on the whole BESS lifetime profitability is not considered.

The battery lifetime is significantly related to the battery chemistry and BESS operation. Recently, Collath et al. [14] have developed an overview about relevant ageing mechanisms as well as degradation modelling approaches, confirming that the effects of degradation, in particular decreasing capacity, increasing resistance, and safety implications, can have significant impacts on the economics of a BESS. In power system techno-economic studies, degradation effect due to battery ageing is mainly modelled either enforcing operational limits [15,16], or using the energy throughput model [7], or employing the cycle-counting model [17]. Since the cycle-counting degradation method is more advanced than the energy throughput method [2], in this work it is adopted the cycle-counting model technique. It relies on the non-linear ageing occurring from battery cycling: cycles with smaller depth-of-discharge (DoD) contributes less than cycles into the degradation of the battery [17]. Each cycle with a certain DoD is assigned with a fixed amount of degradation to the energy capacity according to the cycle depth ageing stress function that can be obtained from the experimental data [2]. The cycle-counting method is incorporated into the optimization framework by including the cost of degradation into the objective function. This cost is calculated by benchmarking the amount of degradation with the battery replacement cost [18]. The cycle-counting degradation model used in this work it is described in the next Section 3.2.5.

Concerning the battery efficiency modelling, the loss in a power-energy model is commonly considered through the introduction of the energy efficiency factor which can be assigned either separately for both charging and discharging operations [19], or as a round-trip efficiency for the whole cycle [20,21]. The generic power–energy model assumes fixed energy efficiencies and constant rated charging/discharging power that do not depend on the battery state of charge, or the rate of charging/discharging current. In this work, a dynamic charge/discharge efficiency is considered in the MINLP optimization framework. This dynamic efficiency depends on the actual battery output power rate. The BESS dynamic efficiency model is described in a detailed way in the next Section 3.2.4.

In conclusion, it is worth noting that in this work historical electricity prices data from CAISO market are considered as input of the optimization model, and the price-taker hypothesis is assumed. Price-taker means that the BESS operations do not affect the electricity prices. In [22] historical (not forecasted) price and demand and a price-taker model were used to assess the economic benefits of deploying energy storage into the New York electricity market. The effect of grid-scale BESS on electricity price formation was studied in [23]. Finally, the strategic behavior of a Li-Ion BESS operator under price uncertainty conditions in day-ahead and real-time electricity markets was examined in [24].

1.2. Aim and novelty of the study

The analysis of the existing literature on BESS modelling in techno-economic studies has revealed a gap regarding proper assumptions about BESS efficiency, lifetime, and degradation. In particular, most linear and non-linear optimization frameworks were not considering a dynamic battery efficiency and a cycle-counting degradation model to account for the changing performance of the battery over time due to its usage and charge/discharge cycles. This includes the variation in energy losses during different operational modes and the impact of ageing on the battery's ability to store and discharge energy effectively. By incorporating dynamic efficiency, the model can adjust battery usage based on real-time efficiency metrics, allowing for more precise control and improved profitability. Similarly, the cycle-counting degradation model accounts for the degradation effects due to varying depths of discharge, enabling a more accurate prediction of the battery's lifespan and overall impact on economic returns. The present work expands on previous literature by developing a new BESS energy arbitrage model which explicitly considers both dynamic efficiency and battery degradation. The computational performance of the proposed power-energy BESS model is analyzed by comparing three Python-based optimization techniques. The scenario with no-degradation is formulated as a linear programming (LP) problem, while the scenarios with and without degradation are formulated as mixed-integer linear programming (MILP), and as mixed-integer non-linear programming (MINLP) problems. The non-linearity is introduced by implementing a BESS dynamic charge/discharge efficiency that is a function of the BESS power rate. Therefore, the linear MILP problem, based on a constant efficiency value, is converted to a non-linear (MINLP) problem based on time-dependent efficiency values. Concerning the degradation due to ageing, a cycle-counting degradation model is used, based upon a semi-empirical degradation function. Finally, a long-term profitability analysis is developed during the whole BESS lifetime considering one end-of-life (EOL) criterion. In this proposed case study, historical electricity market prices from the CAISO electricity market in the United States, California, are used as input. In fact, given that the focus of the paper is on battery dynamic efficiency and degradation, we use the standard and relatively simple assumption of perfect foresight about electricity markets prices. The computational, ageing, and profitability analysis enables the investigation of different scenarios, offering a deeper understanding about their impacts on achievable profit from energy arbitrage and on how BESS operations should be adapted to account for these effects. Within this context, the primary objective of this work is to derive an optimization framework to address the optimal scheduling of a grid-scale BESS while providing energy arbitrage service in the wholesale CAISO electricity market. Consequently, a long-term profitability analysis is conducted based on the BESS optimal scheduling simulated by the optimization model. It is selected the CAISO electricity market for having one of the highest RESs penetration and share of battery storage capacity in the United States [25].

To bridge the identified gap, the present study aims to:

- Establish a powerful and easy-replicable optimization model to maximize the net profit derived by energy arbitrage by optimizing the battery dispatch operations in the wholesale electricity market.
- Evaluate the break-even investment cost where BESS becomes profitable for energy arbitrage by conducting a long-term techno-economic analysis, considering as applicative case the CAISO wholesale electricity market.
- Provide readers and power plant managers with guidelines to incorporate a dynamic efficiency behavior and a cycle-counting degradation model into the optimization model. In this way, it is possible to obtain realistic evaluations of profitability.

The remainder of the work is organized as follows. In Section 2 it is presented the BESS layout and the operating principle of the energy arbitrage optimization problem. Section 3 describes the methodology implemented to build the LP, MILP, and MINLP BESS optimization models, including the dynamic efficiency and the cycle-counting degradation model. Section 4 provides a comprehensive discussion about the results obtained by the computational, ageing and profitability analysis of the proposed energy arbitrage case-study. Finally, conclusions and foreseen next steps are included in Section 5.

2. Battery energy storage system layout

The system under investigation is a Li-ion BESS that provides energy arbitrage service to the electricity grid. A schematic of the system layout, along with the factors considered for net profit evaluations, is provided in Fig. 1. The battery energy storage system, managed by the proposed scheduling energy management system (EMS) model, is comprised of the battery with its battery management system, the DC/AC bidirectional inverter, and the transformer. The energy conversion losses caused by the battery and by the power electronic section (inverter and transformer) are introduced by considering the battery charge/discharge efficiency $\eta_{ch/dh}$, the dynamic inverter efficiency $\eta_{inv}(t)$, and the transformer efficiency η_{tr}. Additionally, the self-discharge losses occurring during charge, discharge, and idle operations are included by $\eta_{self-ch}$, $\eta_{self-dh}$, and $\eta_{self-idle}$, respectively. Starting from the left (Fig. 1), the bi-directional inverter is responsible for converting the DC power flows downstream from the BESS into AC power flows, and vice versa. Then, the transformer is needed to match the voltage levels required by the power distribution grid and BESS. Finally, the AC power flows are exchanged through the grid interface and the energy arbitrage service is simulated. The basic principle of energy arbitrage consists of taking advantage of the electricity price volatility: buying energy at a low price, storing it, and selling it later at a higher price. For this reason, the net profit $\mathbb{P}(t)$ is equal to the export revenue stream $\mathbb{R}(t)$ minus the import cost stream $\mathbb{C}_{imp}(t)$ and the degradation cost stream $\mathbb{C}_{deg}(t)$. A more comprehensive description about the energy conversion losses and the degradation model is reported in Section 3.2.4 and in Section 3.2.5, respectively.

3. Methodology

The problem of finding the most suitable operational strategy for energy arbitrage can be treated as an optimization problem. The LP, MILP, and MINLP optimization BESS models built in this work are based upon the assumption that the BESS owner has perfect foresight of electricity prices, leading to best-case financial returns. Thence, the BESS is assumed to be a price-taker, meaning its activities do not affect the price of energy. However, it is worth noting that previous research on energy arbitrage profits from the PJM market [26,27] suggests that the perfect foresight assumption may lead to overestimation of arbitrage revenue, but by a modest percentage (10–15 %) when compared to simpler strategies that rely on back casting of recent historical prices. Additionally, the model assumes that the battery trades in the real-time electricity market, which provides the best opportunity for energy arbitrage due to its high volatility.

The time resolution of the presented models is $\Delta t = 1\ [h]$, which is the same as the time resolution of the input energy prices used for financial settlement in the CAISO electricity market in the United States. The proposed BESS energy arbitrage models are based on a $T = 168\ [h]$, i.e. one week, scheduling optimization time horizon with a $\Delta t = 1\ [h]$ resolution. This scheduling procedure is repeated each week for one year of dispatch operations. This approach assumes a perfect forecast over one week at a time, mimicking a real working condition where accurate price forecasts typically have a time horizon of less than a week. Fig. 2 illustrates the adopted scheduling mechanism.

The BESS energy arbitrage models presented in this work are developed in a Python environment. Firstly, a linear programming (LP) model is built using the Python library *pulp* [28]. Linear programming means that the mathematical function describing the objective function, as well as the constraints of the system, can all be described as linear combinations of the decision variables, which define the operational strategy of the optimization problem. This first LP model, presented in Section 3.1, was developed to provide a basis for comparison for the next MILP and MINLP models. Furthermore, thanks to this comparison between different optimization frameworks having the same input (hourly CAISO energy prices), it is possible to demonstrate the consistency of the simulated results. Secondly, a mixed-integer linear programming (MILP) model was created. In this case, the model was built using the Python *pyomo* environment [29]. Since in the LP and MILP cases the objective function and the constraints can be formulated as linear combinations of the decision variables, the BESS charge/discharge efficiencies must be assumed to remain constant for each time step *t*. Finally, a mixed-integer non-linear programming (MINLP) model is implemented also in the Python *pyomo* environment [29]: the non-linearity corresponds to introducing a dynamic BESS charge/discharge efficiency that depends upon the actual energy rate of the battery at each time step *t*.

Regarding the degradation effect due to ageing, a cycle-counting degradation model is applied in the MILP and MINLP frameworks. Differently, in the LP model, the degradation penalty cost function is not considered in the objective function. More details about the implemented solvers are presented in Section 4.1, where a computational analysis is performed to compare the different optimization frameworks. The choice of using different optimization frameworks has the goal to compare the obtained simulation results by progressively increasing the degree of complexity and the computational cost, moving from an LP framework to a MILP framework, up to a non-linear MINLP framework.

The following section provides an overview of the energy arbitrage models developed in this work. In Section 3.1 the LP model is presented. In Section 3.2 the MILP/MINLP models are described. We decided to describe the MILP and MINLP model in the same section because the equations implemented are the same, with the only difference being that in the MILP model the efficiency is a constant parameter, while in the

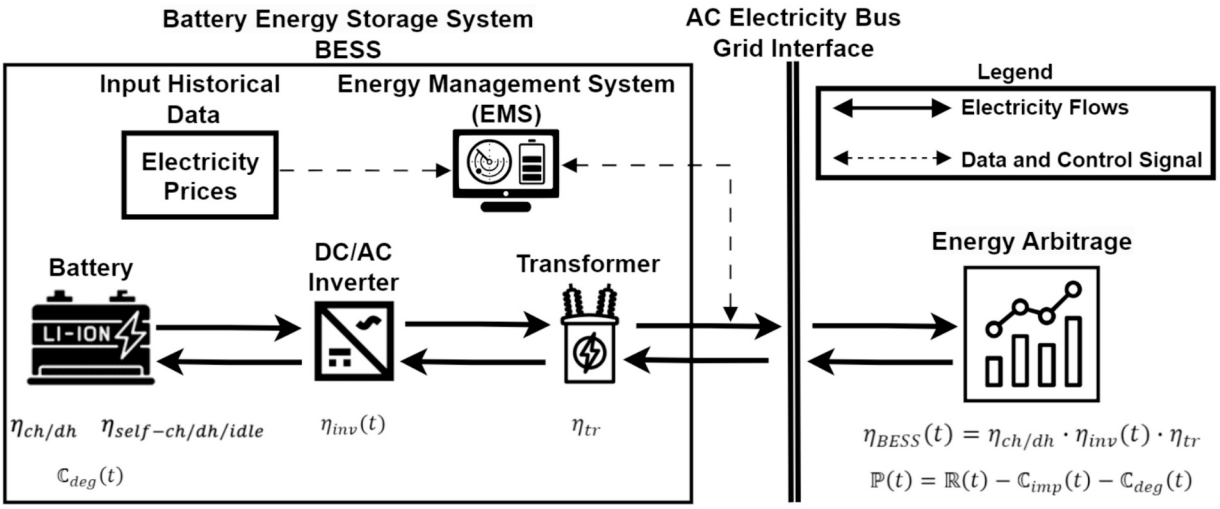

Fig. 1. Schematic layout of the battery energy storage system (BESS), power system coupling, and grid interface components investigated in this work.

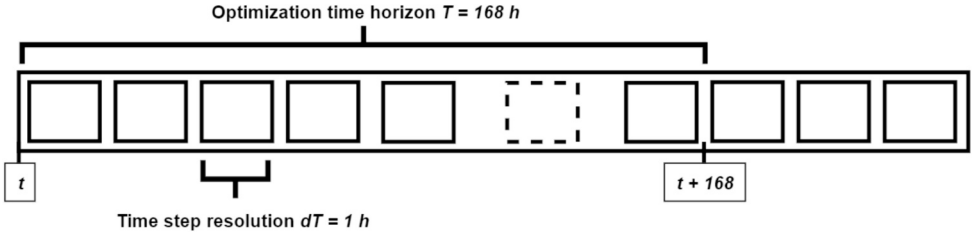

Fig. 2. Schematic diagram of the optimization dispatch approach implemented in the BESS arbitrage models based upon a $T = 168$ $[h]$ scheduling horizon with a $\Delta t = 1$ $[h]$ resolution.

MINLP model the efficiency is a time-dependent variable.

3.1. Linear programming (LP) BESS energy arbitrage model

The LP model presented in this section has the objective to design an optimal operating strategy for a grid-connected battery system with a given set of operational constraints, assuming perfect foresight of electricity prices. The hourly CAISO energy prices of the year 2022 are the locational marginal prices (LMP), which take into account the system marginal price, a congestion cost component and marginal loss component. In this first LP optimization framework, the degradation cost due to ageing and the self-discharge losses are not considered. These losses will be considered later in the more complex MILP and MINLP models. Being a linear model, the charge and discharge efficiencies are assumed to be constant.

3.1.1. LP model: objective function

As described by the objective function defined in Eq. (1), the goal is to maximize the net profit $\mathbb{P}_{LP}(t)$ by netting the revenue $\mathbb{R}_{LP}(t)$ and the import cost $\mathbb{C}_{imp,LP}(t)$ resulting by energy arbitrage, given as input the hourly CAISO energy prices and the BESS parameters.

$$max\{obj\} = max\left\{\sum_{t=1}^{8760}\mathbb{P}_{LP}(t)\right\} = max\left\{\sum_{t=1}^{8760}\mathbb{R}_{LP}(t) - \mathbb{C}_{imp,LP}(t)\right\} \quad (1)$$

The energy arbitrage service consists of buying energy during low price periods, storing it, and selling it later during high-price periods. High price volatility in the local electricity market is thus needed to make this service remunerative. Accordingly, the yearly cumulative revenue $\mathbb{R}_{LP}^{cum}$ and the yearly cumulative import cost $\mathbb{C}_{imp,LP}^{cum}$ are defined in the following Eqs. (2) and (3), respectively.

$$\mathbb{R}_{LP}^{cum} = \sum_{t=1}^{8760}\mathbb{R}_{LP}(t) = \sum_{t=1}^{8760}\lambda_{LMP}(t)\cdot\left[P_{dh,LP}^{bess}(t)\cdot\eta_{BESS,dh,LP}\cdot\Delta t\right] \quad [\$] \quad (2)$$

$$\mathbb{C}_{imp,LP}^{cum} = \sum_{t=1}^{8760}\mathbb{C}_{imp,LP}(t) = \sum_{t=1}^{8760}\lambda_{LMP}(t)\cdot\left[P_{ch,LP}^{bess}(t)\cdot\Delta t \Big/ \eta_{BESS,ch,LP}\right] \quad [\$] \quad (3)$$

From the grid point of view, the revenue is equal to the hourly LMP CAISO energy prices ($\lambda_{LMP}(t)$) times the discharge energy downstream from the BESS inverter. This is the reason why the discharge power is multiplied by the BESS discharge efficiency and by the one-hour time step ($P_{dh,LP}^{bess}(t)\cdot\eta_{BESS,dh,LP}\cdot\Delta t$). Otherwise, the import cost is equal to the hourly LMP CAISO energy prices ($\lambda_{LMP}(t)$) times the charge energy downstream from the BESS inverter. In this case, since the charge power flows in the opposite direction with respect to the discharge power, it is divided by the BESS charge efficiency ($P_{ch,LP}^{bess}(t)\cdot\Delta t/\eta_{BESS,ch,LP}$). The charge power flow $P_{ch,LP}^{bess}(t)$ and the discharge power flow $P_{dh,LP}^{bess}(t)$, expressed in [MW] at each hourly time step t, are the decision variables of the LP problem. These power flows are understood to be converted to energy units in [MWh] through multiplication by the one-hour time step Δt.

3.1.2. LP model: constraints

The next equations (Eqs. (4)–(5)) define the bounds of the charge/discharge power flow. In fact, for each time step t, the charge and discharge power must assume a value within the operating limits of the battery power flow:

$$0 \le P_{ch,LP}^{bess}(t) \le P_{nom}^{bess} \quad \forall t \in T \quad (4)$$

$$0 \le P_{dh,LP}^{bess}(t) \le P_{nom}^{bess} \quad \forall t \in T \quad (5)$$

where P_{nom}^{bess} is the BESS nominal power [MW] corresponding to the maximum charge and discharge power, assumed equal in this work. Additionally, since the battery has limited capacity, one must consider the following operational constraint expressed by Eq. (6):

$$0.2\cdot E_{nom}^{bess} \le \sum_{t=1}^{T} SOC_{LP}(t) + \left[P_{ch,LP}^{bess}(t)\cdot\Delta t\right] - \left[P_{dh,LP}^{bess}(t)\cdot\Delta t\right] \le E_{nom}^{bess} \quad \forall t \in T \quad (6)$$

where $SOC_{LP}(t)$ is the BESS state of charge at each time step t expressed in [MWh], while E_{nom}^{bess} is the BESS nominal capacity in [MWh]. This constraint ensures that the battery energy charge and discharge flows translate into the battery state of charge. It also ensures that the BESS energy content is maintained between the BESS minimum and maximum capacity for each time step t over the time horizon T. A technical minimum of 20 % of the battery nominal capacity is imposed to avoid over-discharge operations that may cause internal failures [30]. The mathematical model considers end of optimization time horizon state-of-charge as an initial condition for next time horizon.

The total BESS efficiency considers the energy conversion losses derived by three electrochemical processes: the battery charge/discharge efficiency $\eta_{ch/dh}$, the inverter efficiency η_{inv} and the transformer efficiency η_{tr}. Since it is assumed a symmetric behavior between charge and discharge phases, the charge and discharge efficiencies are assumed to be the same constant value defined by Eq. (7):

$$\eta_{BESS,ch,LP} = \eta_{ch}\cdot\eta_{inv}\cdot\eta_{tr} = \eta_{BESS,dh,LP} = \eta_{dh}\cdot\eta_{inv}\cdot\eta_{tr} = 0.96\cdot0.98^2\cdot0.98^2 = 0.885 \quad (7)$$

More details about the efficiency values are reported in the next Section 3.2.4.

3.1.3. LP model: simulation set up

Once the LP model is set up with the objective function and all constraints, the next task consists of solve the problem and report back the results. The LP problem solving is performed by introducing a Python-construct function that simulates the BESS operation for energy arbitrage over the course of a year accordingly to the imposed objective function and constraints. The inputs of this function are:

- the initial state of charge at the start of the simulation $SOC_{LP}(t = 0) = 0.5\cdot E_{nom}^{bess}[MWh]$
- the price data frame with the hourly CAISO LMP price $\lambda_{LMP}(t)[\$/MWh]$
- the maximum charge/discharge power capacity set to be equal to P_{nom}^{bess} $[MW]$

- the minimum charge/discharge power capacity set to be equal to 0 $[MW]$
- the maximum charge/discharge energy capacity set to be equal to E_{nom}^{bess} $[MWh]$
- the minimum charge/discharge energy capacity set to be equal to $0.2 \cdot E_{nom}^{bess}$ $[MWh]$
- the constant BESS charge and discharge efficiency $\eta_{BESS,ch,LP} = \eta_{BESS,dh,LP} = 0.885$

After the simulation, the function returns the following outputs with a $\Delta t = 1$ $[h]$ sampling rate:

- the charge and discharge power flows at each hourly time step $P_{ch,LP}^{bess}(t), P_{dh,LP}^{bess}(t)$ $[MW]$
- the state of charge level at each hourly time step $SOC_{LP}(t)[MWh]$
- the timeseries profit $\mathbb{P}_{LP}(t)$, revenue $\mathbb{R}_{LP}(t)$, and import cost $\mathbb{C}_{imp,LP}(t)$ streams [$]

These outputs permit one to examine the yearly BESS dispatch operations and to evaluate in this way the optimal profit derived by energy arbitrage, hence the optimal maximized revenue and the optimal minimized import cost.

3.2. Mixed-integer linear/non-linear programming (MILP/MINLP) BESS energy arbitrage model

The MILP and MINLP BESS energy arbitrage models illustrated in this section have the aim to maximize the BESS profit derived from energy arbitrage over a given time period T, given the historical CAISO hourly energy prices and imposing the BESS operational parameters. As for the LP model, the MILP/MINLP model considers the battery as a price taker and to properly compare them, the same hourly CAISO energy prices of year 2022 are used. Accordingly, a scheduling optimization time horizon of $T = 168$ $[h]$ with a $\Delta t = 1$ $[h]$ resolution is adopted. Differently from the LP model, in this MILP/MINLP optimization framework the degradation cost due to ageing is considered in the objective function. The implemented degradation model is incorporated in the MILP/MINLP BESS model, and it is based on a degradation cost function that evaluates the degradation cost iteratively after each optimization time horizon.

Concerning the BESS charge/discharge efficiency, as before for the LP model, three different efficiencies are considered: the battery efficiency, the inverter efficiency, and the transformer efficiency. Two scenarios are simulated: the former is the MILP scenario based upon the same constant BESS efficiency value considered in the LP model ($\eta_{BESS,ch/dh,\ MILP} = \eta_{ch/dh} \cdot \eta_{inv} \cdot \eta_{tr} = 0.96 \cdot 0.98^2 \cdot 0.98^2 = 0.885$), while the latter is the MINLP scenario which considers a time-dependent dynamic inverter efficiency $\eta_{inv}(t)$ that is a function of the actual energy rate of the battery evaluated at each time step t. In this case, the BESS efficiency is equal to $\eta_{BESS,ch/dh}(t) = \eta_{ch/dh} \cdot \eta_{inv}(t) \cdot \eta_{tr}$. The equations that define this time-dependent efficiency are presented in the following sections that refer to the MINLP scenario. All the equations implemented in the MILP and MINLP models are the same except for the inverter efficiency expression (assumed constant for the MILP case).

3.2.1. MILP/MINLP model: objective function

As reported in Eq. (8), the BESS net profit $\mathbb{P}(t)$ is defined as the algebraic sum of the revenue obtained by exporting energy from the battery to the grid $\mathbb{R}(t)$, the import cost $\mathbb{C}_{imp}(t)$ due to importing energy from the grid to the battery, and the degradation cost due to battery ageing $\mathbb{C}_{deg}(t)$. The import and degradation cost are considered with a minus sign since the goal of the optimization problem is to minimize them, while maximizing the revenue.

$$max\{obj\} = max\left\{ \sum_{t=1}^{8760} \mathbb{P}(t) \right\} = max\left\{ \sum_{t=1}^{8760} \mathbb{R}(t) - \mathbb{C}_{imp}(t) - \mathbb{C}_{deg}(t) \right\} \quad (8)$$

As defined in Eq. (9), the yearly cumulative revenue component $\mathbb{R}^{cum}$ is obtained by multiplying the LMP hourly energy price $\lambda_{LMP}(t)$ with the BESS discharge power $P_{dh}^{bess}(t)$ for reach time step Δt, taking into account the BESS discharge dynamic efficiency $\eta_{BESS,dh}(t)$ and the self-discharge losses occurring during the discharge phase $\eta_{self-dh}$. At the contrary, the yearly cumulative import cost $\mathbb{C}_{imp}^{cum}$ expressed in Eq. (10) is equal to the LMP hourly energy price $\lambda_{LMP}(t)$ multiplied by the BESS charge power $P_{ch}^{bess}(t)$ for each time step Δt, taking into account the BESS charge dynamic efficiency $\eta_{BESS,ch}(t)$ and the self-discharge losses occurring during the charge phase $\eta_{self-ch}$.

Considering now the yearly cumulative degradation cost $\mathbb{C}_{deg}^{cum}$ reported by Eq. (11), it is defined as the sum between the charge and discharge power flow at each time step, multiplied by the degradation coefficient $\mu_{deg,j}$. The battery ageing model implemented in this work is described in Section 3.2.5. As illustrated in Eq. (12), the degradation coefficient represents the slope of the linear approximation of battery ageing, evaluated after each episode j. The time period of every episode j corresponds to the optimization time horizon $T = 168$ $[h]$. The numerator of the degradation coefficient is the difference between the BESS remaining capacity at the start $E_{start,j}^{rem}$ and at the end $E_{end,j}^{rem}$ of the episode j. The remaining capacity expresses the rate of the battery capacity fade based upon the battery charging/discharging frequency and it is evaluated according to the degradation function described in the next Section 3.2.5. Since these components are defined as a percentage of the initial capacity, they are converted into energy terms by multiplying with the BESS nominal capacity E_{nom}^{bess} and by dividing by 100. As defined by Eq. (13), the denominator of the degradation coefficient is the sum between the BESS charge and discharge power flow $P_{tot}^{bess}(t)$ evaluated during the episode j. The degradation coefficient is iteratively updated based upon the degradation results of the last episode j. Therefore, since the time period of every episode j corresponds to the optimization time horizon T, the degradation coefficient assumes a different value after each optimization time horizon ($T = 168$ $[h]$). Finally, the degradation coefficient is multiplied by the BESS penalty cost due to ageing $\mathbb{C}_{pen}^{bess}$, expressed in [$/MWh-year], assuming an end-of-life (EOL) criterion of 80 %. This constant parameter provides an economical value of the battery capacity fade, and it can be interpreted as an annualized cost of replacing the battery after the battery's lifespan.

$$\mathbb{R}^{cum} = \sum_{t=1}^{8760} \mathbb{R}(t) = \sum_{t=1}^{8760} \lambda_{LMP}(t) \cdot \left[P_{dh}^{bess}(t) \cdot \eta_{BESS,dh}(t) \cdot \eta_{self-dh} \cdot \Delta t \right] \quad [\$] \quad (9)$$

$$\mathbb{C}_{imp}^{cum} = \sum_{t=1}^{8760} \mathbb{C}_{imp}(t) = \sum_{t=1}^{8760} \lambda_{LMP}(t) \cdot \left[P_{ch}^{bess}(t) \cdot \Delta t / \left(\eta_{BESS,ch}(t) \cdot \eta_{self-ch} \right) \right] \quad [\$] \quad (10)$$

$$\mathbb{C}_{deg}^{cum} = \sum_{t=1}^{8760} \mathbb{C}_{deg}(t) = \sum_{t=1}^{8760} \mu_{deg,j} \cdot \left[P_{ch}^{bess}(t) + P_{dh}^{bess}(t) \right] \cdot \Delta t \quad (11)$$

$$\mu_{deg,j} = \left\{ \left[\left(\left(E_{start,j}^{rem} - E_{end,j}^{rem} \right) / 100 \right) \cdot E_{nom}^{bess} \right] \Big/ \sum_{t=1}^{T_j} P_{tot}^{bess}(t) \cdot \Delta t \right\} \cdot \left[C_{pen}^{bess} / (1 - EOL) \right] \quad [\$/MWh] \quad (12)$$

$$P_{tot}^{bess}(t) = P_{ch}^{bess}(t) + P_{dh}^{bess}(t) \quad [MW] \tag{13}$$

3.2.2. MILP/MINLP model: continuous constraints

The continuous constraints refer to all those constraints necessary to describe the dispatching operations of the continuous variables of the MILP/MINLP energy arbitrage models. The first constraint defined in Eq. (14) ensures that the battery power discharge flow $P_{dh}^{bess}(t)$ is less than the grid limit P_{grid}^{lim} for all time steps. The grid limit corresponds to the maximum power that the grid can accept at the point of common coupling. The reference power grid limit is set to 10 [MW]. Similarly, the constraints defined by Eqs. (15) and (16) ensure that the battery charge and discharge power flows ($P_{ch}^{bess}(t)$, $P_{dh}^{bess}(t)$) must be higher or equal to the minimum battery power (set equal to zero) and lower or equal to the maximum battery power, namely the battery nominal power P_{nom}^{bess}, for all time steps. The binary variable of charge $\beta_{ch}(t)$ and discharge $\beta_{dh}(t)$ are introduced to prevent charging and discharging from occurring simultaneously, which could otherwise occur during negative prices.

$$P_{dh}^{bess}(t)\cdot\beta_{dh}(t) \le P_{grid}^{lim} \quad \forall t \in T \tag{14}$$

$$0 \le P_{ch}^{bess}(t)\cdot\beta_{ch}(t) \le P_{nom}^{bess} \quad \forall t \in T \tag{15}$$

$$0 \le P_{dh}^{bess}(t)\cdot\beta_{dh}(t) \le P_{nom}^{bess} \quad \forall t \in T \tag{16}$$

The constraint described by Eq. (17) defines the admissible operative window of the state of charge variable, also considering the remaining capacity at the end of the episode j. There is a technical minimum of 20 % of the battery nominal capacity that must be met to avoid over-discharge operations that may cause internal failures [30]. While the constraint of Eqs. (18a) and (18b) is split into parts a and b to account for the first time step, wherein the state of charge variable assumes a predefined value, and for every step greater than one, respectively. This constraint ensures that the battery energy charge and discharge flows translate into the battery state of charge. Here, the self-discharge losses $\eta_{self-idle}$ are considered to take into account the energy conversion losses during idle operations. The mathematical model considers end of optimization time horizon state-of-charge as an initial condition for next time horizon.

$$0.2\cdot E_{nom}^{bess}\cdot\left(E_{end,j}^{rem}\Big/100\right) \le SOC(t) \le E_{nom}^{bess}\cdot\left(E_{end,j}^{rem}\Big/100\right) \quad \forall t \in T \tag{17}$$

$$SOC(t) = 0.2\cdot E_{nom}^{bess}\cdot\left(E_{end,j}^{rem}\Big/100\right) + \left[P_{ch}^{bess}(t)\cdot\Delta t\right] - \left[P_{dh}^{bess}(t)\cdot\Delta t\right] \quad \forall t \in T : t = 0 \tag{18a}$$

$$SOC(t) = SOC(t-1)\cdot\eta_{self-idle} + \left[P_{ch}^{bess}(t)\cdot\Delta t\right] - \left[P_{dh}^{bess}(t)\cdot\Delta t\right] \quad \forall t \in T : t \ge 1 \tag{18b}$$

Eq. (19) defines the battery cycle rate variable $Cyc_{rate}(t)$, namely the fractional cycle-rate with respect to a full cycle during the 1-hour Δt period [13]. One unit of full cycle denotes one full charge (from the minimum to the maximum SOC value) and one full discharge (from the maximum to the minimum SOC value). The constraint expressed by Eqs. (20a) and (20b) allows one to evaluate the cumulative cycle rate step by step. As before, Eq. (20a) refers to the first time step, while (20b) defines the cumulative cycle rate for every step greater than one. The term $cycle_{num}$ is the index used to count the number of cycles performed by the battery.

$$Cyc_{rate}(t) = \left[\left(P_{ch}^{bess}(t) + P_{dh}^{bess}(t)\right)\cdot\Delta t / E_{nom}^{bess}\right]/2 \quad [-] \tag{19}$$

$$Cyc_{rate}^{cum}(t) = Cyc_{rate}(t) + cycle_{num} \quad \forall t \in T : t = 0 \tag{20a}$$

$$Cyc_{rate}^{cum}(t) = Cyc_{rate}^{cum}(t-1) + Cyc_{rate}(t) \quad \forall t \in T : t \ge 1 \tag{20b}$$

Similarly, Eq. (21) defines the normalized power rate $P_{rate}(t)$ variable expressed in per unit terms: it corresponds to the power level of the battery at each time step, divided by the BESS nominal power. This variable is useful to evaluate the dynamic charge and discharge efficiency. In fact, since the dynamic BESS inverter efficiency is a function of the power rate in per unit terms, the constraint defined in Eq. (22) allows one to update the efficiency value for each time step. Therefore, using the Python-construct function *calculate_efficiency*, the dynamic inverter efficiency (considered equal during the charge and discharge processes) is evaluated for each $P_{rate}(t)$ value over the optimization time horizon T. The BESS dynamic inverter function applied in this work is defined in the next Section 3.2.4.

$$P_{rate}(t) = \left[P_{ch}^{bess}(t) + P_{dh}^{bess}(t)\right]/P_{nom}^{bess} \quad [-] \tag{21}$$

$$\eta_{BESS,ch}(t) = \eta_{BESS,dh}(t) = calculate\_efficiency(P_{rate}(t)) \quad \forall t \in T \tag{22}$$

3.2.3. MILP/MINLP: integer constraints

This section presents the integer constraints used in the MILP/MINLP optimization problems. These constraints ensure that the battery can only either charge or discharge at each time step t. For this reason, the binary variable of charge $\beta_{ch}(t)$ and discharge $\beta_{dh}(t)$ are introduced in the MILP/MINLP problem formulations. The binary variable of charge $\beta_{ch}(t)$ assumes the value 1 if the BESS is charging, 0 otherwise. On the contrary, the binary variable of discharge $\beta_{dh}(t)$ assumes the value 1 if the BESS is discharging, 0 otherwise. Additionally, the *bigM* method [31] is implemented to bound the integer constraints. It consists of an extension of the simplex algorithm to problems that contain greater/lower-than constraints. The simplex algorithm is one of the most common methods used for solving MILP/MINLP optimization problems. However, to correctly apply it, the starting point, namely all the variables at the first time step, must be a feasible point of the optimization problem. To obtain this initial feasible solution, it is necessary to add an artificial variable that provides an initial basic feasible solution. The artificial variable is the term *bigM* which refers to a large constant number, in our work we set this equal to 5,000,000; that is, at least two orders of magnitude greater than any feasible value. Therefore, thanks to this method it is possible to correctly introduce inequality constraints, greater-than and lower-than certain values, in the MILP/MINLP optimization problem. In fact, the greater- and lower-than constraints are associated with a large negative and positive constant, respectively, which would not be part of any optimal solution, if it exists. Eq. (23) defines the first integer constraint that is a greater-than inequality constraint considering the BESS charge power flow: if the BESS is discharging ($\beta_{ch}(t) = 0$), the BESS charge power flow $P_{ch}^{bess}(t)$ must be greater than or equal to zero; if the BESS is charging ($\beta_{ch}(t) = 1$), the BESS charge power flow $P_{ch}^{bess}(t)$ must be greater than or equal to a redundant negative lower limit ($-bigM = -5,000,000$) that is at least two orders of magnitude lower than any feasible value.

$$P_{ch}^{bess}(t) \ge 0 - bigM\cdot\beta_{ch}(t) \quad \forall t \in T \tag{23}$$

Differently, the second integer constraint expressed by Eq. (24) is a lower-than inequality constraint always considering the BESS charge power flow: if the BESS is discharging ($\beta_{dh}(t) = 1$), the BESS charge power flow $P_{ch}^{bess}(t)$ must be lower than or equal to zero; on the other hand, if the BESS is charging ($\beta_{dh}(t) = 0$) the BESS charge power flow $P_{ch}^{bess}(t)$ must be lower than or equal to a redundant positive upper limit ($bigM = 5,000,000$) that is at least two orders of magnitude greater than any feasible value.

$$P_{ch}^{bess}(t) \le 0 + bigM\cdot(1 - \beta_{dh}(t)) \quad \forall t \in T \tag{24}$$

The formulation of the third and fourth integer constraints is similar, but they are no longer related to the charge power flow, but instead to the discharge power flow. Eq. (25) defines the greater-than inequality constraint of the discharge power flow: if the BESS is discharging ($\beta_{ch}(t) = 0$), the BESS discharge power flow $P_{dh}^{bess}(t)$ must be greater than or equal to a redundant negative lower limit ($-bigM = -5,000,000$)

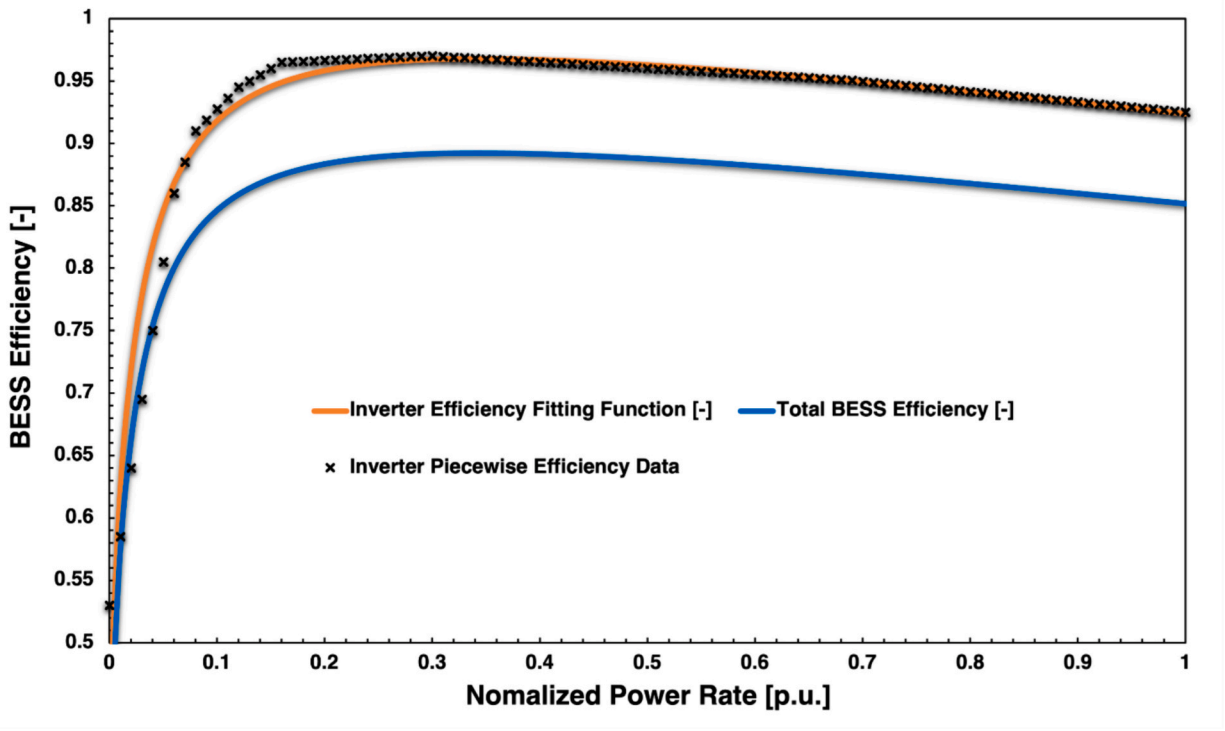

Fig. 3. BESS dynamic efficiency fitting curve as a function of the normalized BESS power rate. (For interpretation of the references to color in this figure, the reader is referred to the web version of this article.)

that is at least two orders of magnitude lower than any feasible value; if the BESS is charging ($\beta_{ch}(t) = 1$), the BESS discharge power flow $P_{dh}^{bess}(t)$ must be greater than or equal to zero.

$$P_{dh}^{bess}(t) \geq 0 - bigM \cdot (1 - \beta_{ch}(t)) \quad \forall t \in T \tag{25}$$

Consequently, Eq. (26) defines the lower-than inequality constraint of the discharge power flow: if the BESS is discharging ($\beta_{dh}(t) = 1$), the BESS discharge power flow $P_{dh}^{bess}(t)$ must be lower than or equal to a redundant positive upper limit ($bigM = -5,000,000$) that is at least two orders of magnitude greater than any feasible value; if the BESS is charging ($\beta_{dh}(t) = 0$), the BESS discharge power flow $P_{dh}^{bess}(t)$ must be lower than or equal to zero.

$$P_{dh}^{bess}(t) \leq 0 + bigM \cdot \beta_{dh}(t) \quad \forall t \in T \tag{26}$$

In conclusion, the last integer constraint expressed by Eq. (27) ensures that for each time step *t,* the sum between the binary variable of charge $\beta_{ch}(t)$ and the binary variable of discharge $\beta_{dh}(t)$ must be lower than or equal to 1. This ensures that the BESS cannot simultaneously charge and discharge at the same time step *t.*

$$\beta_{ch}(t) + \beta_{dh}(t) \leq 1 \quad \forall t \in T \tag{27}$$

3.2.4. MILP/MINLP: BESS dynamic efficiency

Literature tends to neglect the dynamics of efficiency losses and energy conversion losses caused by the battery, the inverter, and the transformer [32]. Firstly, considering the battery section, the battery charging/discharging efficiency is a non-linear function of the battery SOC and battery charge/discharge power. Cao et al. [33] have developed a steady state equivalent circuit model to represent the Li-ion battery efficiency, comprised of an open circuit voltage and three resistors that represent the three main electrochemical process that cause an energy loss: ohmic, charge transfer, and membrane diffusion losses. The study reveals that the battery efficiency slightly improves for higher SOC and lower C-rate. The same result is observed in [34,35]. Accordingly, since the efficiency variation is modest, in this work a constant battery charging/discharging efficiency is assumed with a symmetric efficiency behavior between discharge and charge process. Hence, the charge efficiency is imposed to be equal to the discharge efficiency $\eta_{ch} = \eta_{dh} = 0.96$. Considering now the power electronic section comprised of the inverter and transformer, as proven in [32,36], these components comprise the main cause of energy losses. In addition, they are strongly dependent upon the power output levels, leading to quite low efficiency values (about 50–80 %) for power rates lower than 0.1, while a steadily higher efficiency value (about 90 %) for high power rates with a maximum efficiency at a power rate around 0.3. Typically, battery models developed to optimize energy arbitrage dispatch operations are based upon constant efficiency values. As reported by [2], there have been few studies that have assessed the impact of dynamic efficiency during BESS operations. To address this gap, in this work the empirical BESS inverter efficiency developed by Kim et al. [36] is adopted. We aim to introduce this dynamic behavior to better account for the effects of BESS working conditions on battery efficiency and life expectancy. According to [37], the transformer efficiency is considered constant and equal to $\eta_{tr} = 0.98^2$. As given by Eq. (28), the inverter efficiency model developed in [36] is based upon a piecewise linear approximation depending on the current BESS exchanged power at each time instant *t* as follows:

$$\eta_{inv}(t) = \begin{cases} 5.5 \cdot P_{rate}(t) + 0.53 & if\ 0 \leq P_{rate}(t) \leq 0.06 \\ 2.5 \cdot P_{rate}(t) + 0.71 & if\ 0.06 \leq P_{rate}(t) \leq 0.08 \\ 0.875 \cdot P_{rate}(t) + 0.84 & if\ 0.08 \leq P_{rate}(t) \leq 0.12 \\ 0.5 \cdot P_{rate}(t) + 0.885 & if\ 0.12 \leq P_{rate}(t) \leq 0.16 \\ 0.037 \cdot P_{rate}(t) + 0.959 & if\ 0.16 \leq P_{rate}(t) \leq 0.295 \\ -0.05 \cdot P_{rate}(t) + 0.985 & if\ 0.295 \leq P_{rate}(t) \leq 0.695 \\ -0.082 \cdot P_{rate}(t) + 1.00697 & if\ 0.695 \leq P_{rate}(t) \leq 1 \end{cases} \tag{28}$$

where $P_{rate}(t)$ is the normalized BESS power rate evaluated at each time instant *t* and previously defined in Eq. (21). Since in the *pyomo* environment a non-constant expression cannot be used in a Boolean context (e.g., using an "*if*" statement), the efficiency function previously defined is converted into an explicit form, as defined by Eq. (29):

Table 1
Alpha coefficients, their 95 % confidence bounds (CB) and the goodness-of-statistic parameters (R^2 and *SSE*) of the dynamic BESS inverter fitting function.

R^2	*SSE*	Alpha coefficients (95 % CB)	
0.99553	0.0023938	α_1	0.5992 (0.59, 0.6085)
		α_2	0.02324 (0.02207, 0.02441)
		α_3	−0.1041 (−0.1098, −0.09845)
		α_4	0.4424 (0.4331, 0.4517)

$$\eta_{inv}(t) = \frac{\alpha_1 \cdot P_{rate}(t)}{\alpha_2 + P_{rate}(t)} + \alpha_3 \cdot P_{rate}(t) + \alpha_4 \tag{29}$$

This dynamic BESS inverter efficiency function is obtained by fitting the piecewise efficiency function defined by Eq. (28). A similar fitting expression was adopted in [34,38]. The fitting procedure results are presented in the following Fig. 3. The orange curve corresponds to the inverter piecewise efficiency fitting curve. The black fitted points are obtained by using the inverter efficiency defined by Eq. (28). The four alpha coefficients and their goodness-of-fit statistical parameters (R-squared (R^2) parameter, the sum of squares due to error (*SSE*), and the 95 % confidence bounds (CB)) are reported in Table 1. In Fig. 3 it is also shown that the total BESS efficiency (blue curve), namely the product between the battery efficiency, the variable inverter efficiency, and the transformer efficiency, as defined by the following Eq. (30):

$$\eta_{BESS}(t) = \eta_{ch/dh} \cdot \eta_{inv}(t) \cdot \eta_{tr} \tag{30}$$

Since the introduction of a time-dependent and power-level dependent efficiency make the BESS optimization problem non-linear, it is considered only in the MINLP model. Differently, in the LP and MILP model it is considered a constant value of the inverter efficiency equal to $\eta_{inv,LP/MILP} = 0.98^2$ [37]. As defined by Eq. (31), the total BESS efficiency assumes a constant value of 88.5 %, in accordance with [34,35,37,38]:

$$\eta_{BESS,LP/MILP} = \eta_{ch/dh} \cdot \eta_{inv} \cdot \eta_{tr} = 0.96 \cdot 0.98^2 \cdot 0.98^2 = 0.885 \quad [-] \tag{31}$$

Finally, another energy loss mechanism that occurs during both charge, discharge and idle phase considered in this work corresponds to self-discharge losses [39]. According to [40], self-discharge losses are assumed to be constant during charge, discharge, and idle operations equal to $\eta_{self-ch} = \eta_{self-dh} = \eta_{self-idle} = 99.99\ [\%/h]$. Considering a BESS with a nominal capacity of 2 [MWh], this means that its capacity is reduced by 0.0002 $[MWh]$ per each hour if during this hour it operates at the nominal capacity.

3.2.5. MILP/MINLP: BESS degradation model

The objective function, constraints, and the dynamic efficiency above-mentioned are all contained within the BESS MILP/MINLP Python-construct class and the BESS MILP/MINLP arbitrage optimization Python-construct function. The update of the remaining capacity based on an empirical degradation function occurs outside the BESS MILP/MINLP arbitrage optimization Python-construct function. In fact, degradation is accounted for inside the BESS MILP/MINLP Python-construct class. To perform this updating process, the parameter cyc_{num} is used. The empirical degradation function is defined by the following Eq. (32) and illustrated in Fig. 4. It is defined as a non-linear function with respect to the number of cycles performed by the battery, assuming a 6th-order polynomial behavior having a positive coefficient for the positive exponents, and a negative coefficient for the negative exponent. This equation has been derived by Xu et al. [41]: they proposed a semi-empirical lithium-ion battery degradation model obtained by combining fundamental theories of battery degradation and their observations in battery ageing test results.

The degradation function described above represents the degradation in percentage terms with respect to the initial capacity due to the battery ageing. This function is evaluated recursively after every *j-th* episode. As reported in the zoom of Fig. 4, the time period of every *j-th* episode is equal to the optimization time horizon $T = 168\ [h]$. In this way, it is possible to calculate the remaining capacity at the start $E^{rem}_{start,j}$ and at the end $E^{rem}_{end,j}$ of every *j-th* episode. As previously defined by Eqs. (11), (12), these parameters are used to evaluate the degradation factor $\mu_{deg,j}$ and, consequently, the degradation cost $\mathbb{C}_{deg}(t)$.

The battery capacity decay is assumed to be a 6th-order polynomial function of the number of cycles performed by the battery. Battery degradation is a non-linear process with respect to the current state of life and external stress factors, such as state of charge, number of charge/discharge cycles, depth of charge/discharge, charge/discharge rate, and temperature [41]. The rate of capacity decrease, as a function of number of cycles, is significantly higher during the early cycles than during the later cycles, and then increases rapidly when reaching the end of life (EOL). At this EOL point, also named knee point, the battery degrades remarkably faster, and the remaining lifetime is extremely limited. Consequently, in this study we define one EOL criterion that is reached when the remaining fraction of the battery capacity achieves 80 % of the initial capacity [42,43]. As a result, in the simulations the end of the battery life occurs when the remaining battery capacity reaches the defined EOL value.

3.2.6. MILP/MINLP: Simulation set up

Once the objective function and constraints are set-up, the next section of the MILP/MINLP model consists of effectively perform the optimization process. This procedure is done by introducing a Python-construct function that simulates the BESS operation for energy arbitrage over the course of a year accordingly to the imposed objective function and constraints. More specifically, the inputs parameters are:

- the initial state of charge at the start of the simulation $SOC(t=0) = 0.5 \cdot E^{bess}_{nom}\ [MWh]$
- the price data frame with the hourly CAISO LMP price $\lambda_{LMP}(t)[\$/MWh]$
- the maximum charge/discharge power capacity set to be equal to $P^{bess}_{nom}\ [MW]$
- the minimum charge/discharge power capacity set to be equal to $0\ [MW]$
- the maximum charge/discharge energy capacity set to be equal to $E^{bess}_{nom}\ [MWh]$
- the minimum charge/discharge energy capacity set to be equal to $0.2 \cdot E^{bess}_{nom} \cdot \left(E^{rem}_{end,j}/100\right)\ [MWh]$
- in the MILP model, the constant BESS efficiency value $\eta_{BESS,MILP} = 0.885$
- the initial value of the battery cycle rate variable set to be equal to $Cyc_{rate}(t=0) = 0$
- the initial value of the remaining capacity at the start and the end of the first episode $j = 1$, expressed as a percentage of the BESS capacity, set to be equal to $E^{rem}_{start,j=1} = 100\ [\%]$ and $E^{rem}_{end,j=1} = 0\ [\%]$
- the initial value of the power flow variable used to evaluate the degradation cost, set to be equal to $P^{bess}_{tot}(t=0) = 0$

After the simulation, the function returns the following outputs with a $\Delta t = 1\ [h]$ sampling rate:

$$E^{bess}_{rem}(cyc_{num}) = 100 + 9.30^{-20} \cdot cyc^6_{num} - 1.35^{-15} \cdot cyc^5_{num} + 7.70^{-12} \cdot cyc^4_{num} - 2.52^{-8} \cdot cyc^3_{num} + 3.11^{-5} \cdot cyc^2_{num} - 0.0258 \cdot cyc_{num} \quad if\ 0 < cyc_{num} \leq 3771 \tag{32}$$

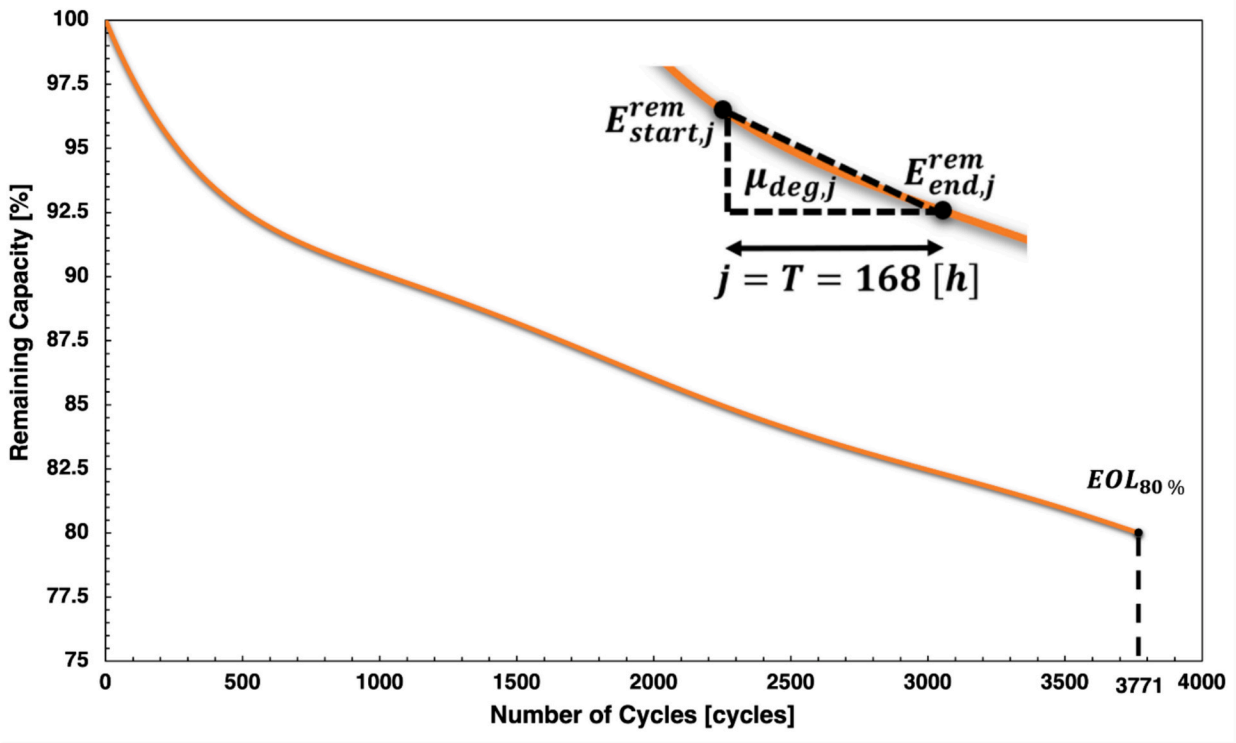

Fig. 4. Empirical degradation function incorporated in the MILP/MINLP optimization problem. It defines the remaining capacity cycle after cycle performed by the BESS. The zoom illustrates the degradation factor $\mu_{deg,j}$ used to evaluate the degradation cost. It is evaluated considering the difference between the BESS remaining capacity at the start $E^{rem}_{start,j}$ and at the end $E^{rem}_{end,j}$ of the *j-th* episode. The time period of every *j-th* episode is equal to the optimization time horizon $T = 168\ [h]$.

- the charge and discharge power flow at each hourly time step $P^{bess}_{ch}(t)$, $P^{bess}_{dh}(t)$ $[MW]$
- the state of charge level at each hourly time step $SOC(t)[MWh]$
- the binary variables of charge $\beta_{ch}(t)$, and discharge $\beta_{dh}(t)$ [0, 1]
- the cumulative cycle rate variable $Cyc^{cum}_{rate}(t)$ $[cyc]$ corresponding to the number of cycles performed by the battery
- the timeseries profit $\mathbb{P}(t)$, revenue $\mathbb{R}(t)$, import cost $\mathbb{C}_{imp}(t)$, and degradation cost $\mathbb{C}_{deg}(t)$ [$]

In addition, concerning the MINLP configuration, the optimization function returns the following outputs always with a $\Delta t = 1\ [h]$ sampling rate:

- the normalized power rate $P_{rate}(t)$ variable expressed in per unit terms [p.u.]
- the timeseries BESS dynamic efficiency variable $\eta_{BESS}(t)$ $[-]$

3.3. LP and MILP/MINLP models: post-processing profitability analysis

The above-mentioned LP and MILP/MINLP models are implemented to simulate the optimal BESS energy arbitrage dispatch operations chronologically over the BESS calendar lifetime T_{BESS}. It is not computationally feasible to solve the LP, MILP/MINLP problems for a time horizon of years [7]. Accordingly, the optimization process based upon the simulation time horizon $T = 168\ [h]$ is recursively repeated each week over one year of BESS operations. In fact, shorter optimization horizons reduce computational load and complexity: this allows the optimizer to better handle the high granularity of hourly price fluctuations and inter-temporal constraints of energy storage efficiently. Furthermore, extending the optimization horizon could enable the battery to operate under a multi-week accumulation strategy, assuming perfect foresight of electricity price trends. However, current forecasting algorithms typically predict electricity prices with reasonable accuracy only up to one week [33]. Extending this to longer periods, while theoretically appealing for maximizing arbitrage opportunities, is currently impractical due to the limitations in predictive accuracy over extended time horizons. For simplicity, it is assumed that the yearly simulated operations continue year by year until the EOL criterion is reached.

In the proposed case study, we used the real-time locational marginal market prices in a specific transmission node in the CAISO market, shown in Fig. 5. For simplicity, the simulation is based on the same market prices, i.e., for the year 2022, for all years of the simulation. In Fig. 6 the hourly CAISO LMP price $\lambda_{LMP}(t)$ for the most profitable week of the year is shown: for most of the hours, the energy prices oscillate in the range of $0 - 200\ \$/MWh$, while between 5500 and 6500 h the price volatility strongly increases reaching a maximum value of about $1400\ \$/MWh$. Before selecting the 2022 price in the CAISO SANTIAGO_6_LN001 transmission node, different years and locations were investigated and evaluated. This selection process (see Supplementary materials) reveals that the most impactful drivers to make energy arbitrage profitable is to have a high price volatility and a high average LMP value. Therefore, we decided to use the current profile of energy prices due to the high price volatility present in the late summer (between 5500 and 65,000 h) and at the end of the year 2022 (after 8000 h), demonstrating in this way its impact on BESS revenue from energy arbitrage operations. Note that the price volatility of this particular CAISO market node can be considered representative of many future market nodes that will be present in highly renewable electric markets.

Concerning now the profitability analysis, the discounted net present value (i.e., not accounting for the investment cost) of the cumulative profit derived by arbitrage over the BESS calendar lifetime T_{BESS} was evaluated according to the following Eq. (33):

$$NPV = \sum_{n=1}^{T_{BESS}} \frac{\mathbb{P}^{cum}_{n} \cdot (1+\gamma)^{n}}{(1+i)^{n}} \quad [\$] \tag{33}$$

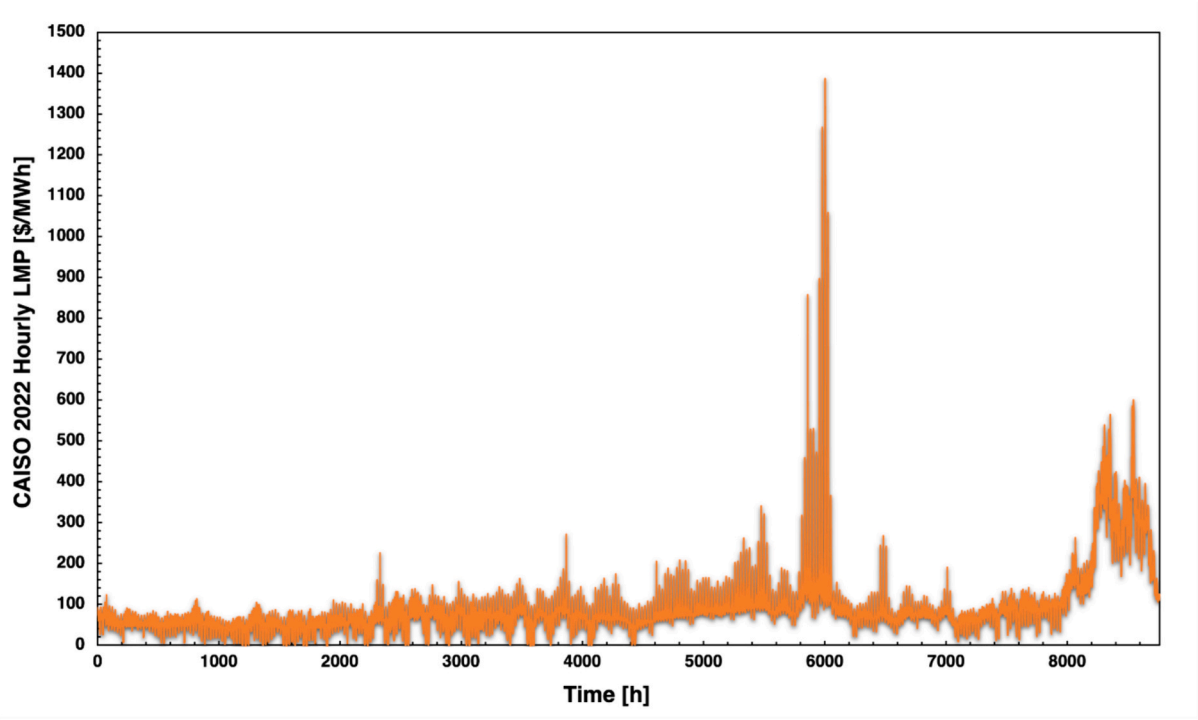

Fig. 5. Hourly locational marginal real-time energy prices in 2022 for the node SANTIAGO_6_LN001 in the CAISO electricity market.
Source: CAISO [44].

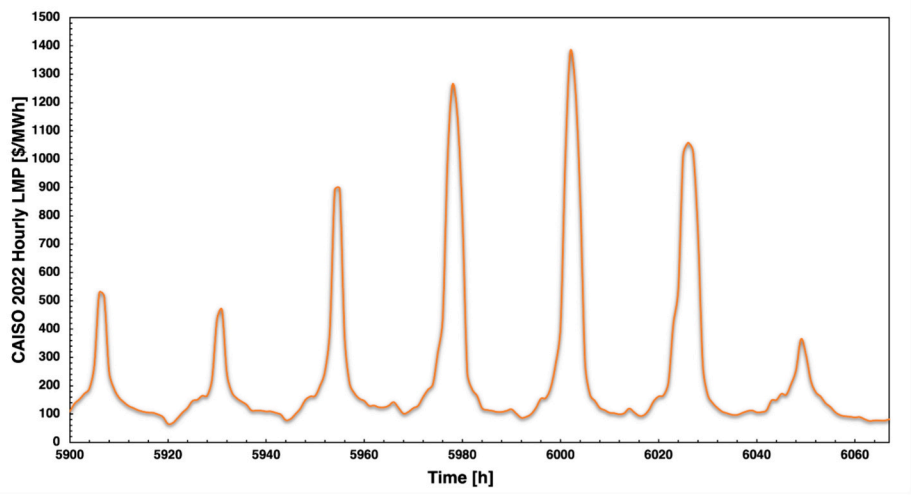

Fig. 6. Hourly locational marginal real-time energy prices for the week Sep/03/2022-Sep/10/2022 for the node SANTIAGO_6_LN001 in the CAISO electricity market.
Source: CAISO [44].

where $\mathbb{P}_n^{cum} = \sum_{t=1}^{8760} \mathbb{P}(t)$ is the yearly BESS operating net profit derived by arbitrage, the subscript n refers to the number of years to reach the EOL criterion, while γ and i are the yearly battery cost escalation rate and the interest rate, respectively. This profitability analysis continues until the EOL criterion is reached.

To effectively evaluate the impact of the net profit stream from energy arbitrage on the net present value, the following parameter defined by Eq. (34) was used as the main comparison metric in the next results section:

$$NPV_{norm} = NPV / E_{nom}^{bess} \quad [\$/MWh] \tag{34}$$

It corresponds to the net present value normalized with respect to the nominal BESS capacity. It can be interpreted as the break-even investment cost where BESS becomes profitable for the given historical energy prices and dynamic dispatch scenario simulated.

4. Results and discussion

This section presents the simulated results obtained by applying the LP, MILP, and MINLP models described in Methodology section. Firstly, in Section 4.1 and in Section 4.2, the results obtained by the computational and ageing analysis were presented. After that, Section 4.3 is focused on the profitability analysis. The results of the computational, ageing and profitability analysis are compared considering the three

different BESS models developed in this work.

4.1. LP, MILP and MINLP performance comparison: computational analysis

This section focuses on analyzing the optimal SOC profile simulated by the LP, MILP, and MINLP BESS models developed in this work. The LP model implements the *pulp* Python package [28]. The MILP model is created using the *pyomo* modelling language integrated with the *gurobi* optimization solver [45]. The Python-based package *pyomo* is an open-source software that supports different optimization capabilities for formulating, solving, and analyzing optimization problems [29]. Finally, a mixed-integer non-linear programming (MINLP) model is tested using the mixed integer non-linear decomposition toolbox in *pyomo*, namely the *mindtpy* solver [46]. This solver allows one to solve MILNP programs using decomposition algorithms. These decomposition algorithms rely upon the combined MILP and MILNP solution: in this work the MILP is solved using *gurobi*, while the MILNP is solved using the interior point optimizer (*ipopt*) solver [47]. As expected, passing from LP and MILP to MINLP framework, the computational cost significantly increases. In fact, the simulation time and the memory usage, measured from the start of the first iteration to the end of the last iteration, passes from about 100 [s] and 5 [MB] in the LP and MILP framework, to about 2500 [s] and 67 [MB] in the MINLP framework.

Fig. 7 compares the LP, MILP, and MINLP BESS optimal dispatching operations simulated during the most profitable week (from Sep/03/2022 to Sep/10/2022). The left vertical axis refers to the simulated SOC profile of the LP (green curve), MILP (black curve), and MINLP (red curve). The orange curve refers to the right axis and corresponds to the CAISO 2022 LMP hourly energy prices occurring during the selected week.

The most interesting aspect highlighted by the data presented in Fig. 7 is understanding how the different models operate to optimize the BESS dispatch operations while providing energy arbitrage services: the battery stores energy (SOC increases, charge phase) during low energy price periods, and releases it (SOC decreases, discharge phase) during high energy price periods. The simulated optimal SOC profile does not record substantial differences amongst the optimization frameworks. As expected, the SOC profile obtained using the LP model (green curve) exploits all the SOC admissible range achieving a value equal to the BESS nominal capacity of 2.0 [MWh], while the MILP (black curve) and MINLP (red curve) configuration presents a more conservative pattern, in fact the SOC when the charging phase is completed reaches about 1.9 [MWh]. This occurs because, as defined previously by Eq. (17), the SOC is limited considering the remaining capacity at the end of the episode j evaluated by the degradation model. This slight difference in the SOC pattern affects the yearly cumulative net profit because the available amount of energy volume that can be exchanged with the grid is lower compared to the LP case.

The cumulative net profit timeseries profile during the year 2022 elaborated by the different programming techniques is presented in Fig. 8. In this work we compare three different models whose result is consistent with each other. This coherence of results represents a cross validation of the models' accuracy and reliability. The consistent outcomes across the linear programming (LP), mixed-integer linear programming (MILP), and mixed-integer nonlinear programming (MINLP) frameworks demonstrate the robustness and generalizability of the proposed models. These results validate the effectiveness of the optimization techniques in capturing the complex dynamics of BESS operations and economics. In fact, since the BESS models are developed in different optimization frameworks, the cumulative net profit, corresponding to the objective function of the optimization problem, presents a similar pattern and a similar final value for all the programming techniques. This consistency across various models underscores the credibility of the results obtained and supports the applicability of the developed frameworks in real-world scenarios. Adopting the LP approach achieves the highest yearly net cumulative profit at time $t = 8760$ [h] of about 46,573 [$/year]. While adopting the MILP and MINLP technique, it is recorded a yearly cumulative net profit of about 41,702 [$] and 38,824 [$], respectively. These results are in accordance with those obtained in [48]. Regarding the cumulative net profit trend over the year 2022, it is evident that a dramatic increase occurs at $t =$

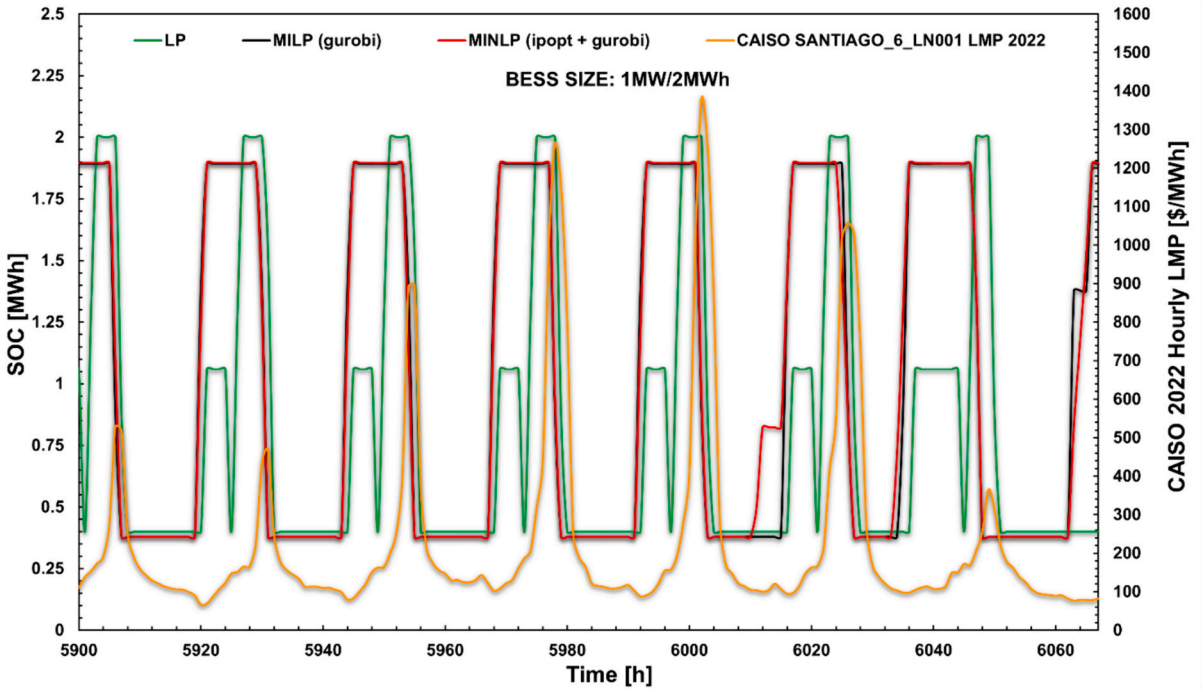

Fig. 7. Optimal BESS dispatch operations during the most profit week (Sep/03/2022-Sep/10/2022). The optimal SOC profiles simulated using the LP (green curve), MILP (*gurobi* solver, black curve), and MINLP (*ipopt* + *gurobi* solver, red curve), refer to the left axis. The right axis represents the CAISO hourly LMP energy prices during the most profit week of year 2022. (For interpretation of the references to color in this figure legend, the reader is referred to the web version of this article.)

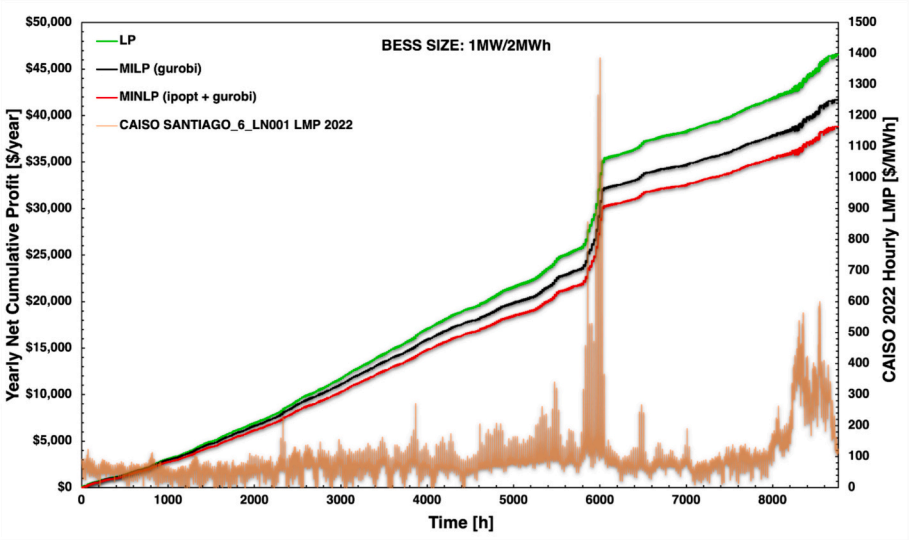

Fig. 8. Optimal net cumulative profit timeseries profile during year 2022. The optimal net profit elaborated using the LP (green curve), the MILP (black curve), and MINLP (red curve) is expressed in $/year, and it refers to the left axis. The right axis represents the CAISO LMP hourly energy prices during year 2022. (For interpretation of the references to color in this figure legend, the reader is referred to the web version of this article.)

6000 $[h]$ and at $t = 8200\ [h]$. This behavior is caused by the highest hourly energy price differences in these periods corresponding to the most profitable weeks of the year (from Sep/03/2022 to Sep/10/2022 and from Dec/21/2023 to Dec/28/2023). This significative result suggests that, since the BESS provides several grid services that generate multiple revenue streams, it is crucial to set a prioritization procedure selecting the most profitable service in the most profitable period established by the market. Therefore, in this specific year, the BESS should provide energy arbitrage in late summer periods and at the end of the year 2022 due to high energy price volatility, while in the remaining part of the year the BESS should provide other grid services (e.g., frequency regulation, load-shifting). To address the issue of multiple services, a possible solution is to consider an optimal multi-temporal dimension able to operate in multiple regimes, e.g., both in real-time and planning operation [49].

4.2. LP, MILP and MINLP performance comparison: ageing analysis

It is noteworthy that in the previous computational analysis section, to properly compare the LP with the MILP/MINLP programming techniques, the degradation cost due to ageing was set equal to zero. This means that the objective function (defined by Eq. (1) for LP and by Eq. (8) for MILP/MINLP) is comprised of only two components, export revenue and import cost. Thus, the implemented optimization procedure aims at maximizing the export revenue stream and to minimize the import cost stream derived by arbitrage. Differently, in the following section the degradation cost is considered in the MILP/MINLP framework. The addition of a new negative component in the objective function constitutes an additional variable that minimizes the degradation cost due to ageing. Consequently, since the degradation is directly linked to the cycle counting process, this added constraint limits the number of cycles per year that the BESS performs to provide energy arbitrage service. This aspect is highlighted in the following Fig. 9, where the LP optimal simulation (no degradation cost scenario and assuming a BESS lifetime of 10 years) is compared to the MILP and MINLP optimal simulations where both scenarios with and without degradation cost are simulated. The comparison is presented for BESS designs that have power-to-energy ratio of 1 MW/1MWh (a) and 1 MW/2MWh (b). Concerning the left axis, the yearly revenue (blue bars), import cost (red bars), degradation cost (black bars), and net profit (green bars) are reported for different assumed values of the battery degradation penalty cost. The right axis shows the number of years to reach the EOL criterion.

The most interesting aspect highlighted by this comparison is that the number of cycles per year simulated by the optimization model progressively decrease by increasing the battery degradation penalty cost. In fact, by introducing a penalty cost in the objective function of the arbitrage optimization model, leads to less cycling of the battery because cycling is prevented from occurring during small energy prices differences. Consequently, this reduction in cycling corresponds to an increase of the number of years to reach the EOL criterion (violet curve). As a result, the maximum value of number of cycles per year in the MILP and MINLP scenario is obtained with a degradation penalty cost set at 0 $/kWh-year: 451 (MILP) and 470 (MINLP) in the 1 MW/1 MW configuration, 410 (MILP) and 395 (MINLP) in the 1 MW/2MWh configuration. Assuming the same trend after the first year simulated, the EOL criterion is reached after about 8.4 years (MILP) and 8.0 years (MINLP) in the 1 MW/1 MW configuration, and after about 9.2 years (MILP) and 9.6 years (MINLP) in the 1 MW/2MWh configuration. At the contrary, the minimum value of number of cycles per year in the MILP scenario is obtained assuming an annualized battery degradation cost of 40 $/kWh-year: about 201 cycles per year in 1 MW/1MWh and 183 cycles per year in the 1 MW/2MWh configuration. The same minimum result assuming an annualized battery degradation cost of 40 $/kWh-year is obtained in the MINLP framework: 192 cycles per year in 1 MW/1MWh and 155 cycles per year in the 1 MW/2MWh configuration. These results highlight the relevance of considering a cycle-counting degradation model in long-term profitability analyses: it is crucial to predict the BESS lifetime and know a priori at which year the battery should be replaced over the entire project lifetime.

4.3. LP, MILP and MINLP performance comparison: profitability analysis

In this section, the normalized net present value (NPV_{norm}), defined by Eq. (34), is illustrated in Fig. 10(a–b) for different battery degradation penalty costs assuming a 1 MW/1MWh (a), and a 1 MW/2MWh (b) configuration. While in Fig. 10(c), the normalized net present value is illustrated for different power-to-energy ratios considering the MILP framework and assuming a constant battery degradation penalty cost of 20 $/kWh-year. The BESS yearly revenue (blue bars), import cost (red bars), degradation cost (black bars), and net profit (green bars) refer to the left axis. While the right axis compares the net present value

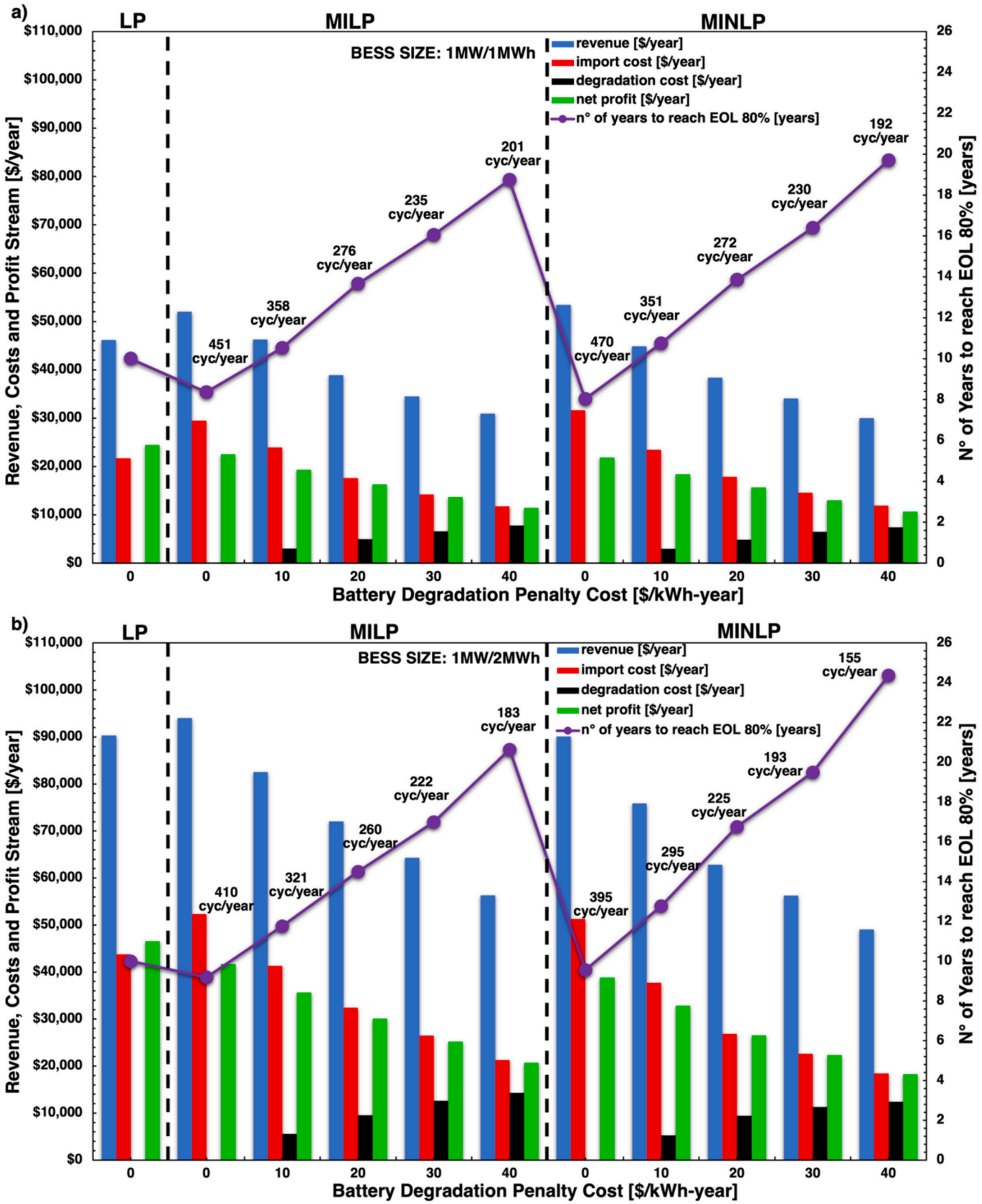

Fig. 9. LP, MILP, and MINLP export revenue stream (blue bars), import cost stream (red bars), degradation cost stream (black bars), and net profit stream (green bars) simulated for different battery degradation penalty cost values expressed in $/kWh-year, considering as power-to-energy ratio 1 MW/1MWh (a) and 1 MW/2MWh (b). The revenue, import cost, degradation cost, and net profit streams refer to the left axis and they are expressed in $ per year. The violet curve represents the number of years to reach the EOL criterion. It refers to the right axis and it is expressed in years. The text in black shows the number of cycles per year. (For interpretation of the references to color in this figure legend, the reader is referred to the web version of this article.)

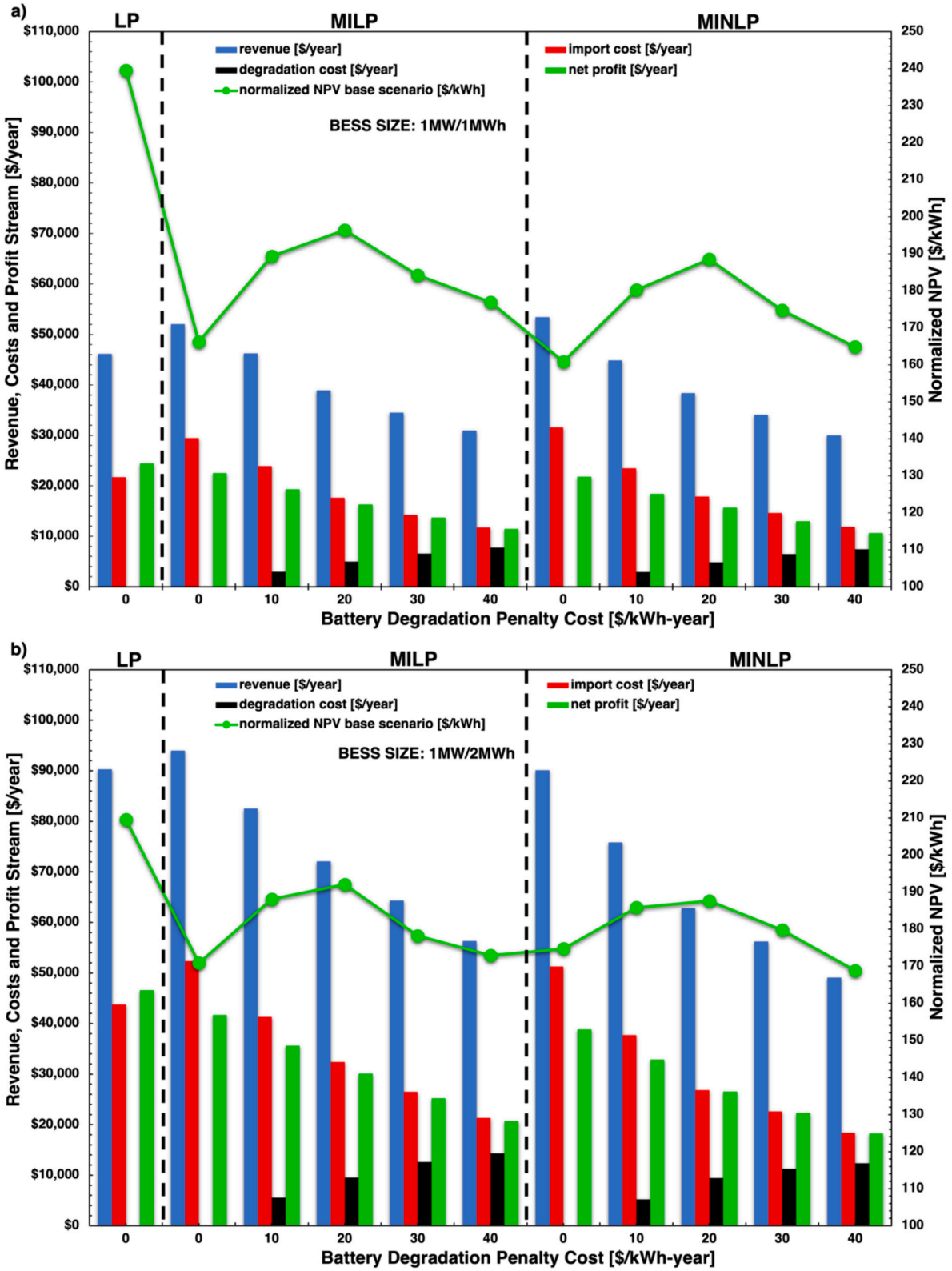

Fig. 10. (a–b): Export revenue (blue bars), import cost (red bars), degradation cost (black bars), and net profit streams (green bars) simulated for different battery degradation penalty cost values expressed in $/kWh-year, assuming as power-to-energy ratio 1 MW/1MWh (a) and 1 MW/2MWh (b). Panel (c): export revenue, import cost, degradation cost, and net profit stream for different power-to-energy ratios, assuming a battery degradation penalty cost of 20 $/kWh-year, and considering the MILP framework. The revenue, import cost, degradation cost, and net profit streams refer to the left axis and they are expressed in $ per year. The green curve represents the normalized NPV evaluated over the number of years after which the EOL criterion is reached. It refers to the right axis and it is expressed in $ per kWh. (For interpretation of the references to color in this figure legend, the reader is referred to the web version of this article.)

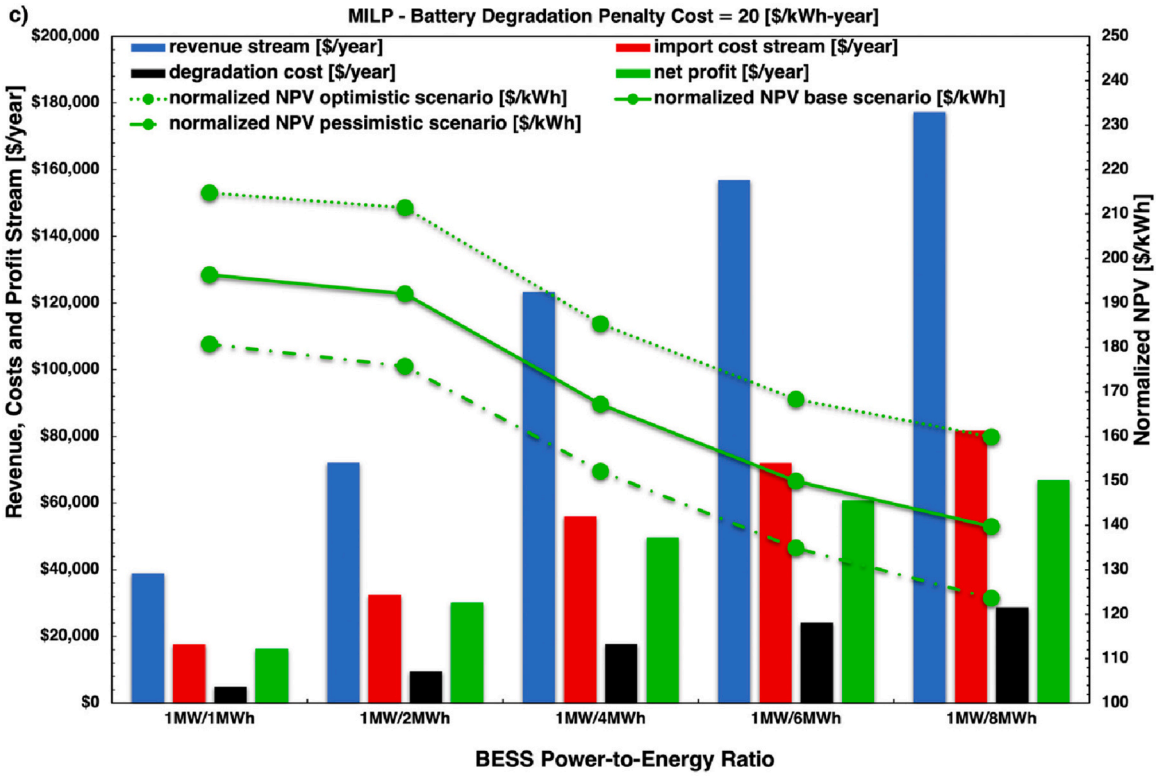

Fig. 10. (*continued*).

normalized with respect the BESS nominal capacity evaluated over the BESS calendar lifetime. Moreover, in Fig. 10(c), three different scenarios are considered: the base scenario (solid green curve) considers an interest rate equal to $i = 6.52\%$ [37], and a yearly battery escalation rate of $\gamma = 4.0\%$. The upper and lower dashed curves refer to the optimistic and pessimistic scenarios, respectively. In the optimistic scenario it is considered an interest rate of $i = 5\%$, while in the pessimistic scenario an interest rate of $i = 8.0\%$.

The results showed in Fig. 10(a–b) confirm that considering a cycle-counting degradation model and therefore a battery penalty cost due to ageing has a strong impact on the NPV of energy arbitrage. In the base scenario ($i = 6.52\%$, $\gamma = 4.0\%$), for a 1 MW/1MWh battery (a), the normalized NPV decreases from 240 $\$/kWh$ (LP, no-degradation case) to 196 $\$/kWh$ (MILP, degradation case with a battery degradation penalty cost of 20 $/kWh-year) and to 189 $\$/kWh$ (MINLP, degradation case with a battery degradation penalty cost of 20 $/kWh-year). Similarly, for a 1 MW/2MWh battery (b), the normalized NPV decreases from 210 $\$/kWh$ (LP, no-degradation case) to 192 $\$/kWh$ (MILP, degradation case with a battery degradation penalty cost of 20 $/kWh-year) and to 188 $\$/kWh$ (MINLP, degradation case with a battery degradation penalty cost of 20 $/kWh-year). In percentage terms, the normalized NPV evaluated in the LP scenario is overestimated on average of about 24.1 % in the 1 MW/1MWh configuration, and about 13.3 % in the 1 MW/2MWh configuration, compared to the MILP and MINLP scenario. In the scenarios where the degradation penalty cost is considered, the highest normalized NPV values of 196 $\$/kWh$ for a 1 MW/1MWh battery, and of 192 $\$/kWh$ for a 1 MW/2MWh battery, are obtained in the MILP layout with a battery degradation penalty cost of 20 $/kWh-year. This value is higher than the case with a degradation penalty cost set at 0 $/kWh where it is obtained a value of 166 $\$/kWh$ (a), and of 171 $\$/kWh$ (b). This trend is due to the introduction of a penalty cost in the objective function that induces less cycling of the battery, thus preserving the BESS lifetime. This longer lifetime due to reduced battery cycling leads to lower profits in the initial BESS operating periods, but over the entire BESS lifetime it has to be considered as an economic advantage. Finally, comparing the MILP and MINLP scenario, no significant differences were found. As a result, since the MILP model is proved more efficient from a computational point of view compared to MINLP, it is implemented in Fig. 10(c) where a sensitivity analysis on BESS capacities is presented.

The results presented were obtained using a fixed time horizon of 168 h. These results may not represent a global optimum if a wider time horizon or a rolling time horizon, as proposed by Abomazid et al. [50], is considered. However, both methods would significantly increase computational time. Therefore, we chose a fixed time horizon to balance robustness and computational efficiency, in accordance with other authors in the literature [7].

In conclusion, concerning the correlation to different power-to-energy ratios illustrated in Fig. 10(c), the normalized NPV decreases with longer charge/discharge times. In the 1 MW/1MWh configuration, it is obtained a normalized NPV of 196 $\$/kWh$ (base scenario), which significantly decreases with longer charge/discharge durations reaching 167 $\$/kWh$ for the 1 MW/4MWh case and 140 $\$/kWh$ for the 1 MW/8MWh case. The NPV reduction from 1 MW/1MWh to 1 MW/8MWh in percentage terms is about 28.9 %.

5. Conclusions and future work

The current work presents a detailed techno-economic profitability analysis on BESS potential revenue from energy arbitrage. A power-energy BESS model with a computationally efficient linear (LP), mixed-integer linear (MILP), and mixed-integer non-linear (MINLP) optimization logic is developed to evaluate the optimal net profit by dispatching a BESS in an arbitrage market. The case-study, based upon historical real-time price data from a location in the CAISO electricity market in the United Sates, shows that considering battery degradation has a significant impact on the achievable NPV from energy arbitrage operation. The normalized NPV (expressed in [$/kWh]) evaluated in this case study can be interpreted as the break-even investment cost where BESS becomes profitable for the given historical prices.

In summary, the profitability analysis shows that, even when assuming no degradation of the battery (LP scenario), the target break-even investment cost with a power-to-energy-ratio of 1 MW/2MWh is 210 $/kWh. Comparing these normalized NPVs to today's battery costs of 300–500 $/kWh [37], demonstrates that investing in BESS for energy arbitrage services only is currently not profitable under the assumptions used in this case study. Alternative locations with higher price volatility and considering a BESS that provides multiple grid services that generate additional revenue streams, could represent valuable strategies to make BESS profitable at today's costs. Furthermore, as projected by the IEA World Energy Outlook 2023 [6], the total BESS investment costs for grid-level applications are forecasted to decrease to <185 $/kWh by 2030 with a long-term goal of 140 $/kWh by 2050. At this 2050 target, the BESS would be profitable at the selected location under the assumption used in this case study. In addition, price volatility in highly renewable electricity markets may increase, which would increase the NPV that BESS could achieve in these future markets even with degradation.

Considering a battery degradation cost via introducing a battery penalty cost in the objective function significantly decreases the normalized NPV compared to the case with no degradation. This reduction in percentage terms in the yearly net profit (or more in general in the normalized NPVs) due to degradation is about 22.4 % in the 1 MW/1MWh case, and about 12.2 % in the 1 MW/2MWh case. Moreover, our analysis illustrates that the cycling of the battery is consistently reduced by adding a battery penalty cost in the objective function of the arbitrage optimization model. Because some BESS degradation inevitably occurs in all systems, a battery penalty cost that accurately characterizes the particular degradation costs of a BESS is crucial.

The results obtained by the BESS optimization models used in this work suggest the relevance of considering battery degradation on BESS profitability analyses. Therefore, the proposed optimization models may present a powerful tool for power plant managers to maximize the net profit derived through energy arbitrage by optimizing the battery dispatch operations and by constantly evaluating and detecting the remaining capacity and degradation.

In future works, we plan to further investigate how to obtain the optimal value of the battery penalty cost as a function of the battery operation and energy market dynamics. In this way, it is possible to capture the complex relationship between degradation and arbitrage profitability. A possible solution could be extending the current optimization model by evaluating the hourly difference energy prices that should activate the BESS operation assuming a specific battery degradation penalty cost. Additionally, by predicting the energy price having as input historical energy prices profile implementing memory models, it would be possible to simulate the BESS operations considering future price signals characterized by high renewables penetration. Finally, we plan to modify the proposed BESS model making it more applicable in real-world context, introducing for instance a renewable power plant integrated with the BESS and grid connected. In this context, it would be worthy to investigate the effect of considering a rolling optimization time horizon instead of the actual fixed optimization time horizon. Moreover, future research could use our modelling approach to simulate a hybrid energy storage system, selecting different storage technologies, tailored to fast and slow grid services provision, respectively.

CRediT authorship contribution statement

Alberto Grimaldi: Writing – original draft, Visualization, Software, Methodology, Investigation. **Francesco Demetrio Minuto:** Writing – review & editing, Methodology, Investigation, Conceptualization. **Jacob Brouwer:** Writing – review & editing, Supervision, Methodology, Conceptualization. **Andrea Lanzini:** Writing – review & editing, Supervision, Methodology, Conceptualization.

Declaration of competing interest

The authors declare the following financial interests/personal relationships which may be considered as potential competing interests: Francesco Demetrio Minuto reports financial support was provided by FSE REACT-EU - PON Ricerca e Innovazione 2014–2020. If there are other authors, they declare that they have no known competing financial interests or personal relationships that could have appeared to influence the work reported in this paper.

Data availability

Data will be made available on request.

Acknowledgements

Francesco Demetrio Minuto carried out this study within the Ministerial Decree no. 1062/2021 and received funding from the FSE REACT-EU - PON Ricerca e Innovazione 2014–2020, Italy. This manuscript reflects only the authors' views and opinions, neither the European Union nor the European Commission can be considered responsible for them.

Appendix A. Supplementary data

Supplementary data to this article can be found online at https://doi.org/10.1016/j.est.2024.112380.

References

[1] F.J. de Sisternes, J.D. Jenkins, A. Botterud, The value of energy storage in decarbonizing the electricity sector, Appl. Energy 175 (2016) 368–379, https://doi.org/10.1016/j.apenergy.2016.05.014.
[2] A.V. Vykhodtsev, D. Jang, Q. Wang, W. Rosehart, H. Zareipour, A review of modelling approaches to characterize lithium-ion battery energy storage systems in techno-economic analyses of power systems, Renew. Sustain. Energy Rev. 166 (2022) 112584, https://doi.org/10.1016/j.rser.2022.112584.
[3] U.S. Energy Information Administration (EIA), Battery Storage in the United States: An Update on Market Trends, U.S. Energy Information Administration (EIA), Washington, DC, USA, 2021 [Online]. Available: https://www.eia.gov/analysis/studies/electricity/batterystorage/pdf/battery_storage_2021.pdf.
[4] U.S. Energy Information Administration (EIA), Preliminary Monthly Electric Generator Inventory, U.S. Energy Information Administration (EIA), Washington, DC, USA, 2022 [Online]. Available: https://www.eia.gov/todayinenergy/detail.php?id=54939 (Accessed: April 27, 2023).
[5] International Energy Agency, World energy outlook 2023 [Online]. Available: https://www.iea.org/reports/world-energy-outlook-2023, 2023.
[6] W. Cole, A. Karmakar, Cost Projections for Utility-Scale Battery Storage: 2023 Update, National Renewable Energy Laboratory, Golden, CO, 2023. NREL/TP-6A40-85332. [Online]. Available: https://www.nrel.gov/docs/fy23osti/85332.pdf.
[7] F. Wankmüller, P.R. Thimmapuram, K.G. Gallagher, A. Botterud, Impact of battery degradation on energy arbitrage revenue of grid-level energy storage, J Energy Storage 10 (2017) 56–66, https://doi.org/10.1016/j.est.2016.12.004.
[8] U.S. Energy Information Administration (EIA), Annual Electric Generator Report, U.S. Energy Information Administration (EIA), Washington, DC, USA, 2021 [Online]. Available: https://www.eia.gov/todayinenergy/detail.php?id=53199 (Accessed: April 27, 2023).
[9] California ISO, Special Report on Battery Storage, Department of Market Monitoring, California Independent System Operator, July 7, 2023 [Online]. Available: https://www.caiso.com/Documents/2022-Special-Report-on-Battery-Storage-Jul-7-2023.pdf.
[10] L. Feng, X. Zhang, C. Li, X. Li, B. Li, J. Ding, C. Zhang, H. Qiu, Y. Xu, H. Chen, Optimization analysis of energy storage application based on electricity price arbitrage and ancillary services, J Energy Storage 55 (2022), https://doi.org/10.1016/j.est.2022.105508.
[11] Y. Hu, M. Armada, M. Jesús Sánchez, Potential utilization of battery energy storage systems (BESS) in the major European electricity markets, Appl. Energy 322 (2022), https://doi.org/10.1016/j.apenergy.2022.119512.
[12] A. Maheshwari, N.G. Paterakis, M. Santarelli, M. Gibescu, Optimizing the operation of energy storage using a non-linear lithium-ion battery degradation model, Appl. Energy 261 (2020), https://doi.org/10.1016/j.apenergy.2019.114360.
[13] H.C. Hesse, V. Kumtepeli, M. Schimpe, J. Reniers, D.A. Howey, A. Tripathi, Y. Wang, A. Jossen, Ageing and efficiency aware battery dispatch for arbitrage markets using mixed integer linear programming, Energies (Basel) 12 (2019), https://doi.org/10.3390/en12060999.

[14] N. Collath, B. Tepe, S. Englberger, A. Jossen, H. Hesse, Aging aware operation of lithium-ion battery energy storage systems: a review, J Energy Storage 55 (2022), https://doi.org/10.14459/2022m.
[15] H. Mohsenian-Rad, Optimal bidding, scheduling, and deployment of battery systems in California day-ahead energy market, IEEE Trans. Power Syst. 31 (2016) 442–453, https://doi.org/10.1109/TPWRS.2015.2394355.
[16] R.L. Fares, M.E. Webber, What are the tradeoffs between battery energy storage cycle life and calendar life in the energy arbitrage application? J Energy Storage 16 (2018) 37–45, https://doi.org/10.1016/j.est.2018.01.002.
[17] B. Xu, Y. Shi, D.S. Kirschen, B. Zhang, Optimal battery participation in frequency regulation markets, IEEE Trans. Power Syst. 33 (2018) 6715–6725, https://doi.org/10.1109/TPWRS.2018.2846774.
[18] B. Xu, J. Zhao, T. Zheng, E. Litvinov, D.S. Kirschen, Factoring the cycle aging cost of batteries participating in electricity markets, IEEE Trans. Power Syst. 33 (2018) 2248–2259, https://doi.org/10.1109/TPWRS.2017.2733339.
[19] Y. Dvorkin, R. Fernandez-Blanco, D.S. Kirschen, H. Pandzic, J.P. Watson, C. A. Silva-Monroy, Ensuring profitability of energy storage, IEEE Trans. Power Syst. 32 (2017) 611–623, https://doi.org/10.1109/TPWRS.2016.2563259.
[20] B. Zhao, A.J. Conejo, R. Sioshansi, Using electrical energy storage to mitigate natural gas-supply shortages, IEEE Trans. Power Syst. 33 (2018) 7076–7086, https://doi.org/10.1109/TPWRS.2018.2850840.
[21] J. Arteaga, H. Zareipour, A price-maker/price-taker model for the operation of battery storage systems in electricity markets, IEEE Trans Smart Grid 10 (2019) 6912–6920, https://doi.org/10.1109/TSG.2019.2913818.
[22] R. Walawalkar, J. Apt, R. Mancini, Economics of electric energy storage for energy arbitrage and regulation in New York, Energy Policy 35 (2007) 2558–2568, https://doi.org/10.1016/j.enpol.2006.09.005.
[23] A.D. Lamont, Assessing the economic value and optimal structure of large-scale electricity storage, IEEE Trans. Power Syst. 28 (2013) 911–921, https://doi.org/10.1109/TPWRS.2012.2218135.
[24] D. Krishnamurthy, C. Uckun, Z. Zhou, P.R. Thimmapuram, A. Botterud, Energy storage arbitrage under day-ahead and real-time price uncertainty, IEEE Trans. Power Syst. 33 (2017) 84–93, https://doi.org/10.1109/tpwrs.2017.2685347.
[25] M. Bolinger, J. Seel, J.M. Kemp, C. Warner, A. Katta, D. Robson, Utility-scale solar, 2023 edition, Lawrence Berkeley National Laboratory, October [Online]. Available: https://emp.lbl.gov/sites/default/files/emp-files/utility_scale_solar_2023_edition_slides.pdf.
[26] R. Sioshansi, P. Denholm, T. Jenkin, J. Weiss, Estimating the value of electricity storage in PJM: arbitrage and some welfare effects, Energy Econ. 31 (2009) 269–277, https://doi.org/10.1016/j.eneco.2008.10.005.
[27] R.H. Byrne, C.A. Silva-Monroy, Estimating the maximum potential revenue for grid connected electricity storage: arbitrage and regulation, in: Tech. Report SAND 2012-3863, Sandia Natl. Lab., 2012.
[28] S. Mitchell, PuLP: A Linear Programming Toolkit for Python, 2011.
[29] M.L. Bynum, G.A. Hackebeil, W.E. Hart, C.D. Laird, B.L. Nicholson, J.D. Siirola, J. Watson, D.L. Woodruff, Pyomo – optimization modeling in Python third edition, Springer optimization and its applications, vol. 67. http://www.springer.com/series/7393.
[30] I. Pavić, N. Čović, H. Pandžić, PV–battery-hydrogen plant: cutting green hydrogen costs through multi-market positioning, Appl. Energy 328 (2022), https://doi.org/10.1016/j.apenergy.2022.120103.
[31] M. Cococcioni, L. Fiaschi, The Big-M method with the numerical infinite M, Optim. Lett. 15 (2021) 2455–2468, https://doi.org/10.1007/s11590-020-01644-6.
[32] M. Schimpe, C.N. Truong, M. Naumann, A. Jossen, H.C. Hesse, J.M. Reniers, D. A. Howey, Marginal costs of battery system operation in energy arbitrage based on energy losses and cell degradation, in: 2018 IEEE International Conference on Environment and Electrical Engineering and 2018 IEEE Industrial and Commercial Power Systems Europe, EEEIC/I CPS Europe, 2018, pp. 1–5.
[33] J. Cao, D. Harrold, Z. Fan, S. Member, T. Morstyn, D. Healey, K. Li, Deep reinforcement learning based energy storage arbitrage with accurate lithium-ion battery degradation model, IEEE Transactions on Smart Grid 11 (5) (September 2020). https://ieeexplore.ieee.org/document/9061038.
[34] C. Betzin, H. Wolfschmidt, M. Luther, Electrical operation behavior and energy efficiency of battery systems in a virtual storage power plant for primary control reserve, International Journal of Electrical Power and Energy Systems 97 (2018) 138–145, https://doi.org/10.1016/j.ijepes.2017.10.038.
[35] G. Rancilio, A. Lucas, E. Kotsakis, G. Fulli, M. Merlo, M. Delfanti, M. Masera, Modeling a large-scale battery energy storage system for power grid application analysis, Energies (Basel) 12 (2019), https://doi.org/10.3390/en12173312.
[36] R.K. Kim, M.B. Glick, K.R. Olson, Y.S. Kim, MILP-PSO combined optimization algorithm for an islanded microgrid scheduling with detailed battery ESS efficiency model and policy considerations, Energies (Basel) 13 (2020), https://doi.org/10.3390/en13081898.
[37] V. Viswanathan, K. Mongird, R. Franks, X. Li, V. Sprenkle, R. Baxter, 2022 Grid Energy Storage Technology Cost and Performance Assessment, 2022.
[38] A. Grimaldi, F.D. Minuto, A. Perol, S. Casagrande, A. Lanzini, Ageing and energy performance analysis of a utility-scale lithium-ion battery for power grid applications through a data-driven empirical modelling approach, J Energy Storage 65 (2023), https://doi.org/10.1016/j.est.2023.107232.
[39] M. Schimpe, M. Naumann, N. Truong, H.C. Hesse, S. Santhanagopalan, A. Saxon, A. Jossen, Energy efficiency evaluation of a stationary lithium-ion battery container storage system via electro-thermal modeling and detailed component analysis, Appl. Energy 210 (2018) 211–229, https://doi.org/10.1016/j.apenergy.2017.10.129.
[40] L. Novoa, R. Flores, J. Brouwer, Optimal renewable generation and battery storage sizing and siting considering local transformer limits, Appl. Energy 256 (2019), https://doi.org/10.1016/j.apenergy.2019.113926.
[41] B. Xu, A. Oudalov, A. Ulbig, G. Andersson, D.S. Kirschen, Modeling of lithium-ion battery degradation for cell life assessment, IEEE Trans Smart Grid 9 (2018) 1131–1140, https://doi.org/10.1109/TSG.2016.2578950.
[42] T.C. Bach, S.F. Schuster, E. Fleder, J. Müller, M.J. Brand, H. Lorrmann, A. Jossen, G. Sextl, Nonlinear aging of cylindrical lithium-ion cells linked to heterogeneous compression, J Energy Storage 5 (2016) 212–223, https://doi.org/10.1016/j.est.2016.01.003.
[43] S.B. Peterson, J. Apt, J.F. Whitacre, Lithium-ion battery cell degradation resulting from realistic vehicle and vehicle-to-grid utilization, J. Power Sources 195 (2010) 2385–2392, https://doi.org/10.1016/j.jpowsour.2009.10.010.
[44] California ISO Energy [Online]. Available: https://www.caiso.com/Pages/default.aspx (Accessed: April 27, 2023).
[45] L. Gurobi Optimization, Gurobi optimizer reference manual [Online]. Available: https://www.gurobi.com, 2023 (Accessed April 27, 2023).
[46] MindtPy Solver [Online]. Available: https://pyomo.readthedocs.io/en/stable/contributed_packages/mindtpy.html (Accessed: April 27, 2023).
[47] Ipopt Solver [Online]. Available: https://coin-or.github.io/Ipopt/ (Accessed: April 27, 2023).
[48] California ISO, 2021 Annual Report on Market Issues & Performance, Department of Market Monitoring, California Independent System Operator, July 27, 2022 [Online]. Available: https://www.caiso.com/Documents/2021-Annual-Report-on-Market-Issues-Performance.pdf.
[49] S. Hanif, M.J.E. Alam, R. Kini, B.A. Bhatti, J.C. Bedoya, Multi-service battery energy storage system optimization and control, Appl. Energy 311 (2022), https://doi.org/10.1016/j.apenergy.2022.118614.
[50] A.M. Abomazid, N.A. El-Taweel, H.E.Z. Farag, Optimal energy management of hydrogen energy facility using integrated battery energy storage and solar photovoltaic systems, IEEE Trans Sustain Energy 13 (2022) 1457–1468, https://doi.org/10.1109/TSTE.2022.3161891.